

STRUCTURAL AND FUNCTIONAL PROPERTIES OF NMDA RECEPTORS IN THE MOUSE BRAIN ENDOTHELIAL CELL LINE bEND3

By

Christopher F. Dart

A thesis submitted to the Faculty of Graduate Studies of
The University of Manitoba
in partial fulfillment of the requirements of the degree of

MASTER OF SCIENCE

Department of Pharmacology and Therapeutics
University of Manitoba
Winnipeg, MB

Copyright © 2010

ABSTRACT

Changes in local cerebral blood flow in response to neural activity is termed functional hyperemia. Previous work in our laboratory indicates that the diameter of brain arteries and arterioles can be increased by N-methyl-D-aspartate (NMDA) receptor activation. We hypothesized that brain endothelial NMDA receptors are responsible for this activity. We looked for expression of NMDA receptors and endothelial cell responses to NMDA receptor agonists and antagonists in the immortalized mouse brain endothelial cell line bEnd.3.

Using RT-PCR and Western blotting we found evidence supporting the presence of NMDA receptor subunits NR1 and NR2C. Functionally, treatment of bEnd.3 cells with combinations of 100 μ M glutamate and D-serine significantly increased intracellular calcium, but the magnitude of these increases was smaller than the expected response from our positive control for nitric oxide (NO) dependent vasodilation, acetylcholine. In agreement, we saw no direct evidence that NO was produced in response to NMDA receptor activation using the Griess method. We did observe an NMDA receptor-dependent increase in protein nitrosylation. This increase is unlikely related to enhanced NO levels since it was not correlated with NO production and was not inhibited by the endothelial NO synthase inhibitor L-NIO. Overall, our data indicate that bEnd.3 cells express functional NMDA receptors and that

activation of these receptors leads to oxidative stress but not eNOS-dependent
NO production.

ACKNOWLEDGMENTS

I would like to start off by thanking Dr. Christopher Anderson for accepting myself as a graduate student under his supervision. This work would not have been possible without his encouragement and guidance. I would also like to extend special thanks to other members of the Anderson lab including Shao Zongjun (June), Jill LeMaistre, Waylon Hunt and Amit Kamboj for their help in answering my questions.

Other members in the Department of Neurodegenerative Disorders that had a significant impact on my research, however directly or indirectly, include Dr. Paul Fernyhough, Dr. Ben Albenzi, Dr. Gordon Glazner, Garry Odero, Solmaz Nafez, Jason Schapansky, Eli Kwaku Akude, Elena Zherebitskaya and Kelly Jorundson.

My time in Winnipeg and the research opportunities afforded to me were made possible through funding by the Department of Neurodegenerative Disorders Studentship, funding from the Manitoba Health Research Council, Canadian Institutes of Health Research and the Faculty of Graduate Studies.

People who helped me survive the cold, frigid, subarctic winters while making the pleasant summers a bajillion times more enjoyable include my dear friends John-Erik Schellenberg-Kochos, Benilda Zamora, Ezgi Öğütçen, Cassidy Erdelyan, Matt Sposito, Nate Lo, Liam McGillivray, Lyndsay Houston, Wes Simmonds, a half-million Chris' at the Nerd Store and Kus.

Support from friends abroad that constantly reminded me there was a world outside of Winnipeg are Curtis Dart, my parents Robert and Patricia Dart, Steven and Renee Little, Sherman Farahani, and Vanessa Hong.

Special thanks to Tara Vicars for playing some 200+ games of Scrabble with me from across the world in Africa. Forgive me for not traveling with you.

TABLE OF CONTENTS

ABSTRACT	ii
ACKNOWLEDGMENTS	iv
LIST OF FIGURES	viii
LIST OF TABLES	ix
LIST OF ABBREVIATIONS	x
INTRODUCTION	
1.1 Regulation of Brain Blood Flow	1
1.2 Regulation of Vascular Tone by Neurotransmitters	4
1.3 Regulation of Vascular Tone by Astrocytes	6
1.4 NMDA Receptors	9
1.5 Non-Neuronal Distribution of NMDA Receptors	18
1.6 Nitric Oxide and Nitric Oxide Synthase	20
1.7 Implications of Neurovascular Dysfunction in Dementia	23
1.8 Rationale	25
1.9 Hypothesis and Objectives	28
MATERIALS AND METHODS	
2.1 Culture of bEnd.3 Cells	29
2.2 Preparation of Protein Extracts	29
2.3 Western Blotting	30
2.4 Calcium Imaging	32
2.5 Polymerase Chain Reaction	33
2.6 Nitric Oxide Assay	37

2.7	Slot Blotting.....	38
2.8	Statistical Analysis.....	39
RESULTS		
3.1	bEnd.3 Cells Express mRNA for NMDAR Subunits.....	40
3.2	bEnd.3 Cells Express NMDAR NR1 and Other Subunits.....	41
3.3	Treatment of bEnd.3 Cells with Glutamate ± D-Serine Causes no Significant Increase in Nitrite Production.....	43
3.4	Treatment with Glutamate and D-Serine Causes an Increase in S-Nitrosylated Protein Dependent on NMDAR Activity.....	45
3.5	S-Nitrosylation is Not eNOS Related.....	48
3.6	Glutamate and D-serine Elicit Small Changes in Intracellular Calcium Levels.....	49
DISCUSSION.....		53
CONCLUSION.....		59
REFERENCES.....		60

LIST OF FIGURES

Figure 1: Neurovascular Blood Supply.....	3
Figure 2: Substances Known to Modulate NMDA Receptor Activity.....	10
Figure 3: Schematic Representation of NR1 Splice Variants.....	11
Figure 4: Formation of NMDA Receptors.....	17
Figure 5: Membrane Domains of NMDA Receptors.....	18
Figure 6: Schematic Representation of the Neurovascular Unit.....	25
Figure 7: PCR Amplification of NMDAR Subunit mRNAs Isolated From bEnd.3 Cells and Whole Mouse Brain.....	41
Figure 8: Western Blot Probing of NMDARs.....	42
Figure 9: Nitrite Production in bEnd.3 cells 24 and 48 ours Post- Treatment with Glutamate or Combination of Glutamate and D-Serine.....	44
Figure 10: Protein S-Nitrosylation in bEnd.3 Cells \pm mGluR/Kainate Receptor Antagonist.....	46
Figure 11: Protein S-Nitrosylation in bEnd.3 Cells \pm NMDAR Antagonist.....	47
Figure 12: Protein S-Nitrosylation in bEnd.3 Cells \pm eNOS Antagonist.....	48
Figure 13: Calcium Response of bEnd.3 Cells to Positive Controls.....	51
Figure 14: Calcium Response of bEnd.3 Cells to Glutamate and D- Serine Treatment.....	52

LIST OF TABLES

Table 1.	NR2-Specific NMDAR Antagonists.....	15
Table 2.	Number of Cycles, Temperatures and Times Used for PCR Amplification of cDNA.....	31
Table 3.	NMDA Receptor Subunit Primers and Expected Product Sizes Used in PCR Analysis.....	34
Table 4.	Antibodies used in Western Blot Probing.....	36

LIST OF ABBREVIATIONS

A β	Amyloid-beta
ACh	Acetylcholine
AD	Alzheimer 's disease
AJ	Adherens Junction
AMPA	amino-3-hydroxy-5-methyl-4-isoxazolepropionic acid
β -ME	β -mercaptoethanol
BBB	Blood-brain barrier
BSA	bovine serum albumin
CNS	Central Nervous System
D-ser	D-serine
DMEM	Dulbecco's modified Eagle's medium
EDTA	2-[2-(Bis(carboxymethyl)amino)ethyl-(carboxymethyl)amino]acetic acid
ER	endoplasmic reticulum
FBS	fetal bovine serum
glu	glutamate
GPCRs	G-protein coupled receptors
HEPES	N-2-Hydroxyethylpiperazine-N'-2-Ethanesulfonic Acid
HRP	horse radish peroxidase
IC ₅₀	inhibitory concentration 50%

LTD	Long-term depression
LTP	Long-term potentiation
NMDA	N-methyl-D-aspartate
NMDARs	N-methyl-D-aspartate receptors
NO	Nitric Oxide
NOS	Nitric Oxide Synthase
PBS	Phosphate Buffered Saline
PCR	polymerase chain reaction
PVDF	polyvinylidene difluoride
RT-PCR	reverse transcription PCR
SDS	sodium dodecyl sulfate
SDS-PAGE	sodium dodecyl sulfate – polyacrylamide gel electrophoresis
TBS	Tris-buffered saline solution
TBST	Tris-buffered saline solution, 0.1% Tween-20
TJ	Tight Junction

INTRODUCTION

1.1 Regulation of Brain Blood Flow

Accounting for only 2% of normal human body weight the brain is responsible for over 20% of daily metabolic needs. The brain is a heterogeneous collection of neurons, astrocytes, microglia, pericytes, microvascular smooth muscle and endothelial cells that all have different energy requirements that must be met. Maintenance of an adequate supply of energy substrates and oxygen through blood vessels is essential to brain function and neuronal survival. Short interruptions in cerebral blood flow can lead to widespread neuronal death within minutes (Hossmann, 2006).

Cerebral blood flow is regulated by two mechanisms: cerebrovascular autoregulation and functional hyperemia. Cerebrovascular autoregulation is responsible for the prevention of harmful increases in cerebral blood flow due to systemic changes in arterial blood pressure. This will not be discussed in great detail. Local changes in cerebral blood flow in response to elevated neuronal activity and corresponding increases in oxygen consumption and glucose utilization is termed functional hyperemia (Iadecola and Nedergaard, 2007). Functional hyperemia was first described in the late 1800's by Roy and Sherrington (Roy and Sherrington, 1890) and forms the basis for today's functional magnetic resonance imaging (fMRI) (Raichle et al., 1975). The blood supply for the brain begins at the circle of Willis located at the base of the brain

(Hossmann, 2006). From here arteries travel along the surface of the brain giving rise to pial arteries (figure 1). Pial arteries are responsible for two-thirds of cerebrovascular resistance, which is unique compared to other organs where vascular resistance is controlled from vessels located within the organ (Faraci and Heistad, 1990). Pial arteries branch into smaller vessels (arteries and arterioles) that penetrate deep into the brain parenchyma (Raichle et al., 1975). Characteristically, these arteries and arterioles are composed of an endothelial layer surrounded by one or more layers of smooth muscle cells whose main responsibility is to control the diameter of these blood vessels. These penetrating arteries and arterioles are separated from the brain substance by an extension of the subarachnoid space, termed the Virchow-Robin space (Jones, 1970). As arterioles reach deeper into the brain the basal lamina comes into direct contact with astrocytic endfeet, at which point they become intracerebral arterioles. Arterioles give rise to capillaries, which are comprised solely of a single layer of endothelium resting on the basal lamina, and pericytes. Pericytes are a type of cell with contractile capabilities purported to be involved in functions related to maintenance of the blood brain barrier (BBB) integrity and angiogenesis (Fisher, 2009). Arterioles and capillaries are responsible for the remaining third of vascular resistance observed in the brain (Faraci and Heistad, 1990).

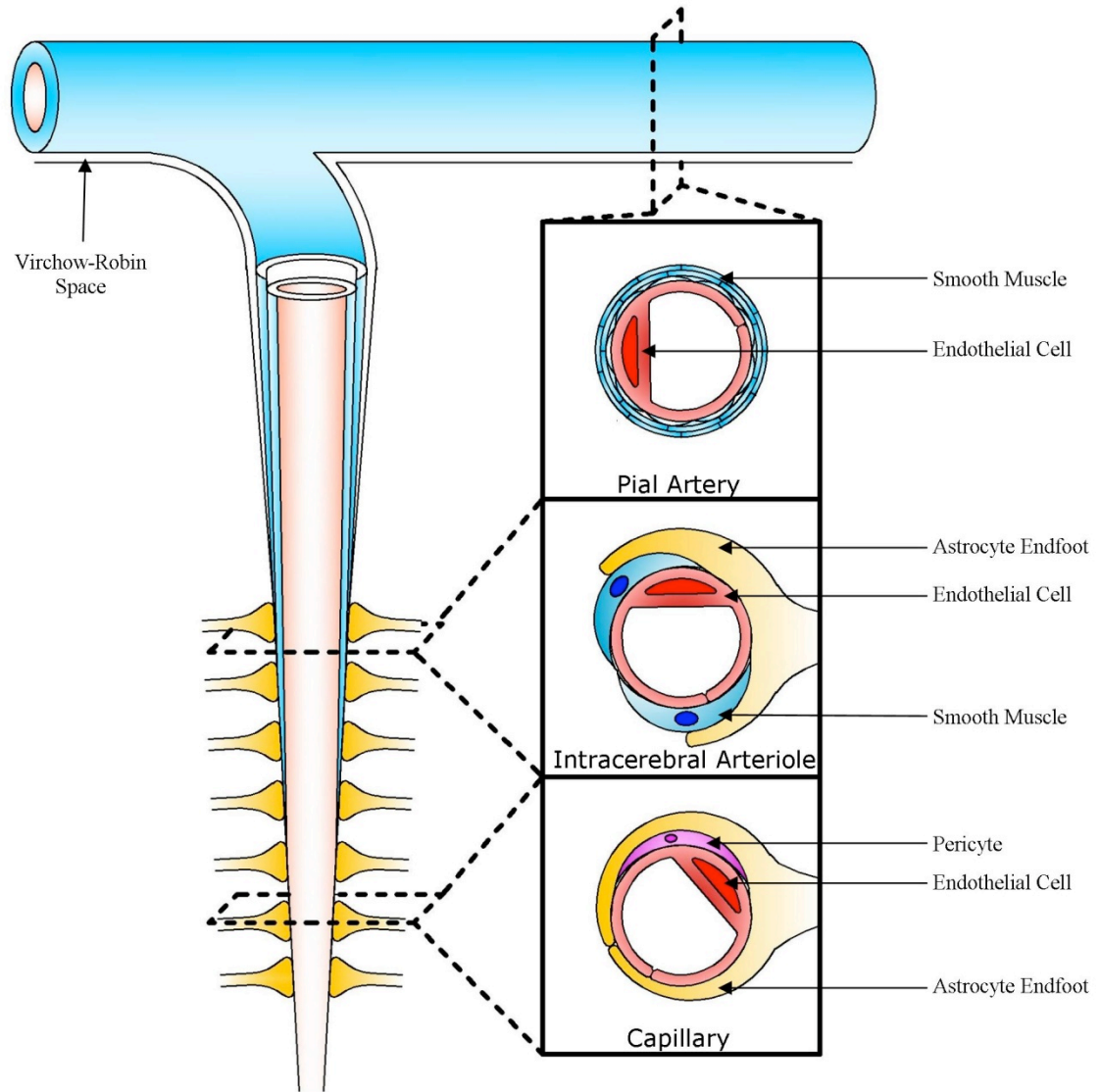


Figure 1. Neurovascular Blood Supply. Local blood supply to regions within the brain originates from pial arteries that travel along the surface of the brain. Pial arteries consist of a layer of endothelial cells wrapped in several layers of smooth muscle cells. These vessels are separated from the brain matter by the Virchow-Robin space. As arteries penetrate further into the cerebral tissue they become intracerebral arterioles. Like the pial arteries they also consist of a layer of endothelium though are often only ensheathed by a single layer of smooth muscle. Astrocytic endfeet come into direct contact with the basement membrane of the vessels. Astrocytes maintain contact with blood vessels as they continue to narrow becoming capillaries. Capillary diameter is controlled by pericytes, which are small contractile cells similar in function to smooth muscle.

1.2 Regulation of Vascular Tone by Neurotransmitters

As metabolic demands of tissues increase, the supply of oxygen and energy substrates to the sites of activity must increase accordingly. Increased supply of oxygen and nutrients by a responsive increase in local blood flow is termed functional hyperemia. The overall spatial and temporal mechanisms involved are unclear but we do know of several mechanisms driven by neuronal activity that influence cerebrovascular tone and blood flow. To meet the highly dynamic metabolic needs of the brain, both regionally and locally, a variety of nerve terminals are believed to play a role in functional hyperemia. The vascular supply of the brain is innervated by both the sympathetic and parasympathetic nervous system in addition to sensory nerves (Gulbenkian et al., 2001). Sympathetic nerves from the superior cervical ganglion have a high density of contacts on the pial arteries that dissipate as vessels penetrate deeper into the brain parenchyma, though some can still be detected in arterioles (Gulbenkian et al., 2001). Stimulation of adrenergic nerves results in vasoconstriction of pial arteries and a reduction of cerebral blood supply (Raichle et al., 1975). Other signal substances released from sympathetic nerve endings include ATP and neuropeptide Y (Gulbenkian et al., 2001). Cholinergic parasympathetic neurons originate from the sphenopalatine ganglion and innervate the pial arteries (Suzuki and Hardebo, 1993). Electrical stimulation of these nerves in rats was found to induce NO-dependent relaxation that was

blocked by tetrodotoxin (Toda et al., 1995). Tetrodotoxin antagonizes voltage-gated fast sodium channels, whose actions are principally responsible for regulating sodium influx into these NO producing cells following membrane depolarization (Liu et al., 2000). NO is a fat soluble radical that has the ability to diffuse across cell membranes with a short half-life of about 5 seconds (Archer, 1993).

In addition to autonomic innervation, central innervation has also been observed. Other aminergic neurons believed to be involved in modulating blood flow include dopamine (Krimer et al., 1998), which constricts both microvessels and capillaries in the brain, γ -aminobutyric acid (GABA) and serotonin.. GABAergic neurons release GABA, which in turn dilates blood vessels through a GABA_A-receptors. Serotonergic neurons have been reported to have both vasoconstrictory and vasodilatory effects, which is attributed to the large and complex number of serotonin receptors distributed in neurons and astrocytes (Drake and Iadecola, 2007).

NO is thought to play a pivotal role in functional hyperemia in the brain. NADPH-diaphorase staining is a technique that positively identifies NOergic neurons. Staining of neuron populations in the brain show that most NADPH-diaphorase positive cells lie nthe basal lamina covering endothelial cells and pericytes (Wiencken and Casagrande, 2000). In the cerebellum, stellate cells express neuronal nitric oxide synthase (nNOS) (Rodrigo et al., 1994) and

release NO and cause vasodilation in response to the neurotransmitter glutamate via N-methyl-D-aspartate receptors (NMDARs). Overall, functional hyperemia is dependent on nNOS to varying degrees regionally. In mice lacking nNOS there was a significant reduction in cerebral blood flow after upper lip stimulation while under anesthesia. Positron electron imaging measuring blood flow and glucose utilization following administration of an nNOS inhibitor showed a pronounced reduction in cerebellar blood flow when the forepaws of anesthetized cats were electrically stimulated. There is some, though less evidence that endothelial NO in the brain has a role in functional hyperemia.

1.3 Regulation of Vascular Tone by Astrocytes

Prior to the late 1970's glial cells were generally accepted to be structural cells that acted as insulation for neurons (Somjen, 1988). Research into receptors present on the cell surfaces of glia began to change this prevailing thought. Beginning in 1978 cultured glial cells were shown to express functional G-protein coupled receptors (GPCRs) that played a role in a diverse array of intracellular signaling (McCarthy and de Vellis, 1978; Van Calker et al., 1978). Some believed that the expression of GPRCs was a culture artifact as opposed to *in vivo* expression however this is not supported by the demonstration that glia, both *in vivo* and *in situ*, maintained expression of GPCRs (Porter and McCarthy, 1997). The first description of a role for

astrocytes in functional hyperemia was made by Newman *et al.* (1984), who described a process by which potassium released across synaptic terminals of active neurons was siphoned through astrocytes and released from astrocytic endfeet onto nearby blood vessels (Newman *et al.*, 1984), causing release of EDHF and vasodilation. A seminal observation that astrocytes can directly influence local arteriole diameter was made by Zonta *et al.* in 2003. These authors demonstrated that a neuronally-induced rise in intracellular astrocyte calcium levels triggered the release of arachidonic acid metabolites from endfeet to reduce vascular tone (Zonta *et al.*, 2003). Astrocytes are well-suited to translate messages from synapses to local vasculature. They have numerous processes that encircle neuronal synaptic terminals. Astrocyte processes also completely ensheath arterioles and capillaries. In addition, perisynaptic astrocyte processes possess other receptors that respond to neurotransmitter release, including glutamate receptors. This structure provides a signaling circuit linking neurotransmission with the blood supply. Moreover, connections associated with nearby neural cells (Bushong *et al.*, 2002; Halassa *et al.*, 2007) occupy mutually exclusive 3-D spaces and are linked by gap junctions to form intricate spatial networks. This provides for upstream and downstream spatial coordination of functional hyperemia signals. One way this is thought to happen is by the phenomenon known as calcium wave propagation during which glutamate induces the development of transient increases in

intracellular calcium, which in turn trigger rises in Ca^{2+} in nearby astrocytes in a wave-like manner (Cornell-Bell et al., 1990). Astrocyte Ca^{2+} waves are propagated by signaling pathways involving gap junctions (Stout et al., 2002), P2X7 ATP receptors and several types of anion channels (Anderson et al., 2004; Darby et al., 2003).

Astrocytic processes contacting arteriolar smooth muscle or basal lamina are capable of releasing vasoactive substances such as the vasoconstrictor cytochrome P450 metabolite 20-hydroxy-(5Z,8Z,11Z,14Z)-eicosatetraenoic acid (20-HETE; Mulligan and MacVicar, 2004) and vasodilatory arachidonic acid metabolites prostaglandin E_2 (PGE_2 ; Hirase, 2005) and epoxyeicosatrienoic acid (EET; Harder et al., 1998). Whether dilatory or constrictor substances are released appears to depend on the prevailing energy status of the local tissue, as dictated by local lactate accumulation (Gordon et al., 2008). *In vivo* experiments involving the photolysis of caged Ca^{2+} in anesthetized adult mice demonstrated a direct relation between the rise in intracellular calcium localized in astrocyte endfeet, vasodilation and increased blood flow proximal to the transients (Takano et al., 2006). Further *in vivo* experiments involving 1,4,5-trisphosphate (InsP_3) uncaging in astrocytes demonstrated that endfoot rises in calcium are dependent on release from intracellular calcium stores from the ER and that vasodilation of vessels near the affected endfoot was propagated to adjacent arterioles (Straub et al., 2006).

Another response mediated by increases in intracellular calcium stores is the exocytotic release of gliotransmitters. Gliotransmitters are chemical mediators released from astrocytes. The major gliotransmitters released in this fashion include glutamate (Bezzi et al., 1998; Parpura et al., 1994), ATP (Coco et al., 2003; Li et al., 2008) and D-serine (Mothet et al., 2005; Schell et al., 1995). D-Serine is a unique gliotransmitters as it is produced almost exclusively in astrocytes. The extracellular concentration of D-serine in a healthy brain is between 5-10 μM (Hashimoto et al., 1995). D-serine has been shown to affect neuronal excitability (Yang et al., 2003) and synaptic plasticity (Yang et al., 2003) and is critical for neural cell development (Kim et al., 2005). D-serine released may bind to the D-serine/glycine co-agonist binding site of NMDAR-type glutamate receptors (Mothet et al., 2000). Whether D-serine affects cerebrovascular tone or brain blood flow is currently unknown.

1.4 NMDA Receptors

N-Methyl-D-Aspartate receptors (NMDARs) are ligand-gated cation channels and are a part of the larger family of ionotropic glutamate receptors including α -amino-3-hydroxy-5-methyl-4-isoxazolepropionic acid (AMPA) and kainate receptors. All characteristically bind the agonist glutamate, which leads to activation of the channel allowing the passage of small cations including Na^+ , K^+ and Ca^{2+} . Influx of ions through these channels can generate

neuronal action potentials. There are several distinguishing properties of neuronal NMDARs that make them unique when compared to other ionotropic receptors: 1) they require an additional co-agonist, either glycine or D-serine, to function and 2) they are normally blocked by Mg^{2+} ions located within the channel pore. Membrane depolarization must occur in order to repel Mg^{2+} from the channel. Other substances which are known to interact with NMDARs and modulate their activity include zinc cations, protons, polyamines such as dizocilpine (MK-801; Ransom and Stec, 1988) and the psychotropic drug phencyclidine (PCP; figure 2).

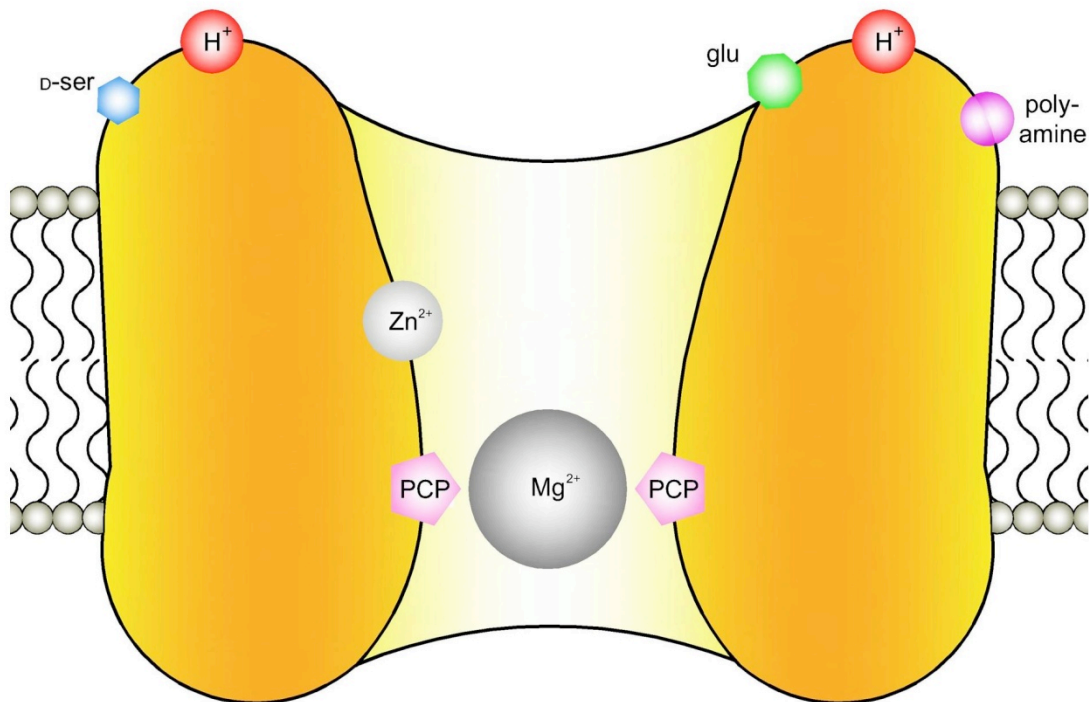


Figure 2: Substances known to modulate NMDA receptor activity. Substances that bind NMDARs with modulatory effects include magnesium (Mg^{2+}), phencyclidine (PCP), zinc (Zn^{2+}), protons (H^+), polyamines and the NMDA receptor agonists glutamate (glu) and D-serine (D-ser).

NMDARs are heterotetrameric protein complexes assembled from a pool of three different gene families, NR1, NR2 and NR3 (Dingledine et al., 1999). The NR1 subunit is essential in all functional NMDARs. It possesses the binding site for regulatory glycine/D-serine (Kuryatov et al., 1994) and is necessary in the formation of tetrameric NMDAR channels (McIlhinney et al., 2003). mRNA for the NR1 subunit is alternatively spliced to form 8 variants (figure 3).

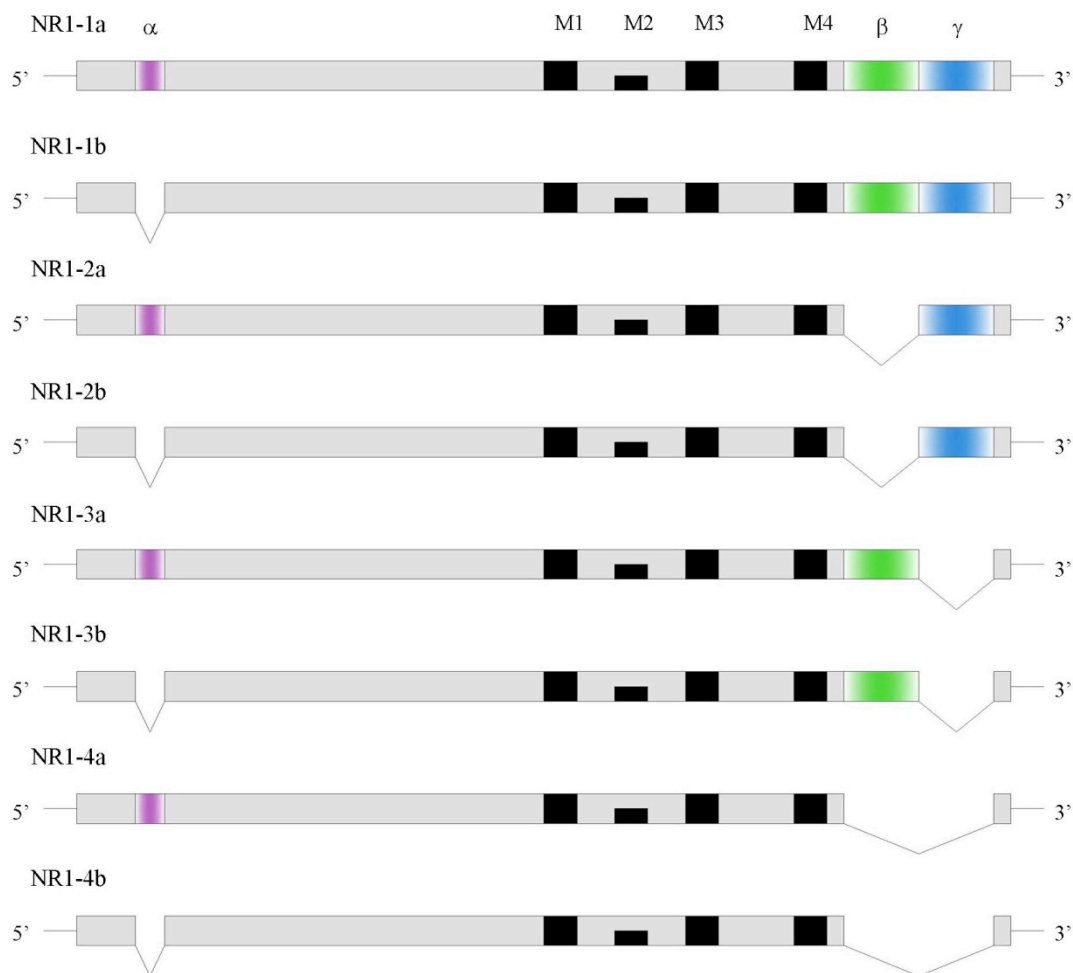


Figure 3. Schematic Representation of NR1 Splice Variants. There are 8 different variants of NR1 resulting from alternative splicing of mRNA. Hydrophobic segments of the NR1 subunit are indicated as black boxes within the gene and are numbered according to their transmembrane domains (M1, M2, M3, M4). M2 is the reentrant loop. The N-terminal deletion α is labeled in purple and the two C-terminal deletions β and γ are labeled in green and blue respectively.

An N-terminal splice site at exon 5 and C-terminal splice regions at exons 21 and 22 are responsible for the variants observed. N-terminal and C-terminal splice variants exhibit altered functional characteristics. NMDARs lacking exon 5 display an increased affinity for NMDA and marked potentiation by spermine (Durand et al., 1993). Variants containing the N-terminal exon 5 express an ER retention motif RRR, which may be suppressed by the PDZ-domain expressed in NR1 subunits containing exon 22 (Standley et al., 2000) thus altering the surface expression of NR1. Exon 5 containing units also exhibit an increased IC_{50} for voltage-independent Zn^{2+} inhibition (Traynelis et al., 1998). C-terminal splice variants are involved in altered phosphorylation states by protein kinase C (Tingley et al., 1993) for enhanced translocation from the ER. Variant C-terminal expression also changes NMDAR targeting to different subcellular structures (Zukin and Bennett, 1995).

The four NR2 subunits (NR2A-D) possess the binding sites for the neurotransmitter glutamate (Anson et al., 1998; Anson et al., 2000; Laube et al., 1998). They are expressed differentially in areas throughout the brain where they combine with NR1 subunits to form functional receptors. Diversity in the NR2 subunit composition of NMDARs affects channel properties such as channel conductance (Momiya et al., 1996), sensitivity to extracellular Mg^{2+} blockage (Qian et al., 2005; Shiokawa et al., 2010), glutamate affinity (Monyer et al., 1994; Vicini et al., 1998; Wyllie et al., 1998) and modification of synaptic

plasticity (Liu et al., 2004). The NR2 subunits are strong candidates for pharmacological treatment due to their differences in tissue distribution and function (Cull-Candy et al., 2001). Successes in the field of pharmacology for successful drug development that target individual subunits such as traxoprodil (CP101,606), a specific NR2B receptor antagonist that has shown promise in phase 2 clinical trials for the treatment of major depression (Preskorn et al., 2008). Other drugs that are known to target NR2 subunits to varying degrees can be seen in Table 1 (Brimecombe et al., 1998; Donevan and McCabe, 2000; Hrabetova et al., 2000; Ilyin et al., 1996; Kew et al., 1998; Kleckner et al., 1999; Traynelis et al., 1995; Williams, 1993).

The four different NR2 subunits show a distinct distribution in the central nervous system that changes expression profile through the course of development (Monyer et al., 1994; Standaert et al., 1996; Watanabe et al., 1994). In neurons NR2B, and to a lesser extent NR2D, predominate in early stages of development. These are gradually replaced by NR2A and the NR2C subunits. At adulthood the NR2A subunit is found expressed ubiquitously throughout the brain while the NR2B and NR2C subunits are at high levels in the forebrain and cerebellum respectively (Kohr, 2006). The multiple functional roles of NR2-containing NMDARs can be further evidenced by contrasting the roles of two of the more common NR2 subunits: NR2A and NR2B. Long-term potentiation (LTP) and long-term depression (LTD) mediated by NMDARs is

believed to be critically important in learning and memory (Kemp and Bashir, 2001). Recent investigations into the differential role of NR2A and NR2B in LTP and LTD have shown that NR2A containing receptors are required for LTP while LTD is moreover controlled by NR2B (Liu et al., 2004; Massey et al., 2004). NR2B containing channels are also believed to play a part in alcohol dependence (Nagy, 2004) and plays a role in chronic inflammatory pain sensation (Hu et al., 2009).

Substance	Mode of Action	Subunit Selectivity	Reference
Ifenprodil	Non-competitive inhibition of NR2B	NR2B>>2A/2B>>2D=2C=2A	(Williams, 1993)
Haloperidol	Non-competitive inhibition of NR2B	NR2B>>2A/2B>>2D=2C=2A	(Ilyin et al., 1996)
Ro 8-4304	Non-competitive inhibition of NR2B	NR2B>2A	(Kew et al., 1998)
CP 101,606	Non-competitive inhibition of NR2B	NR2B>>2C=2A	(Brimecombe et al., 1998)
Felbamate	Non-competitive inhibition of NR2B	NR2B>>2C=2A	(Kleckner et al., 1999)
Conantokin-G	Competitive inhibition of NR2B	NR2B>2D=2C=2A	(Donevan and McCabe, 2000)
D-CPPene	Competitive inhibition of NR2A and 2B	NR2B=2A>2D=2C	(Hrabetova et al., 2000)
PPDA	Competitive inhibition of NR2C and 2D	NR2C=2D>2A=2B	(Hrabetova et al., 2000)
Zn ²⁺	Non-competitive inhibition of NR2A	NR2A>2B>2C	(Traynelis et al., 1995)

Table 1. NR2-specific NMDAR antagonists. Substances shown to exhibit a degree of subunit-specific selectivity for NR2 in recombinant NMDARs. Symbols in subunit selectivity rank orders indicating roughly one (>) or two (>>) orders of magnitude difference in reported IC₅₀

Less is known about the more recently discovered class of NR3 subunits (NR3A-B) and their role in functional NMDARs. Like the NR1 subunit, NR3 contains a binding site for regulatory glycine/D-serine (Yao and Mayer, 2006). They also share similarities with NR2C and NR2D containing receptors insofar as assemblies consisting of an NR3 group tend to exhibit low single-channel conductance (Das et al., 1998). NMDARs containing NR3 subunits have been found impermeable to calcium ions and are also resistant to magnesium-dependent blockade (Chatterton et al., 2002).

Assembly of functional NMDARs is thought to occur in a two-step process. The first step involves dimerization between an NR1 subunit and either an NR2 or NR3. In a second step two heterodimers of either NR1/NR2 or NR1/NR3 further dimerize to form the final active tetrameric channel (Schuler et al., 2008). Thus, all functioning NMDARs consist of two NR1 subunits and two additional units, either trihetero-oligomers consisting of 2NR1:NR2:NR3 (Madry et al., 2007) or homoheterodimers of NR2 (Dingledine et al., 1999) or NR3 (Awobuluyi et al., 2007; Cavara et al., 2009; Madry et al., 2007; Smothers and Woodward, 2007; figure 4). Prior to receptor expression at cellular surface sites a disulfide bridge involving cysteine 79 must be formed between two neighboring NR1 subunits (Papadakis et al., 2004). Each subunit is a transmembrane protein with 3 transmembranous loops (M1, M3 and M4) and one reentrant loop (M2) formed in the intracellular membrane. The M2 loop is

responsible for formation of the channel pore (Bennett and Dingledine, 1995; Wo and Oswald, 1995; Wood et al., 1995). The N-terminal domain of each protein exists on the extracellular side of cells with the C-terminus exposed to the cytosol (figure 5).

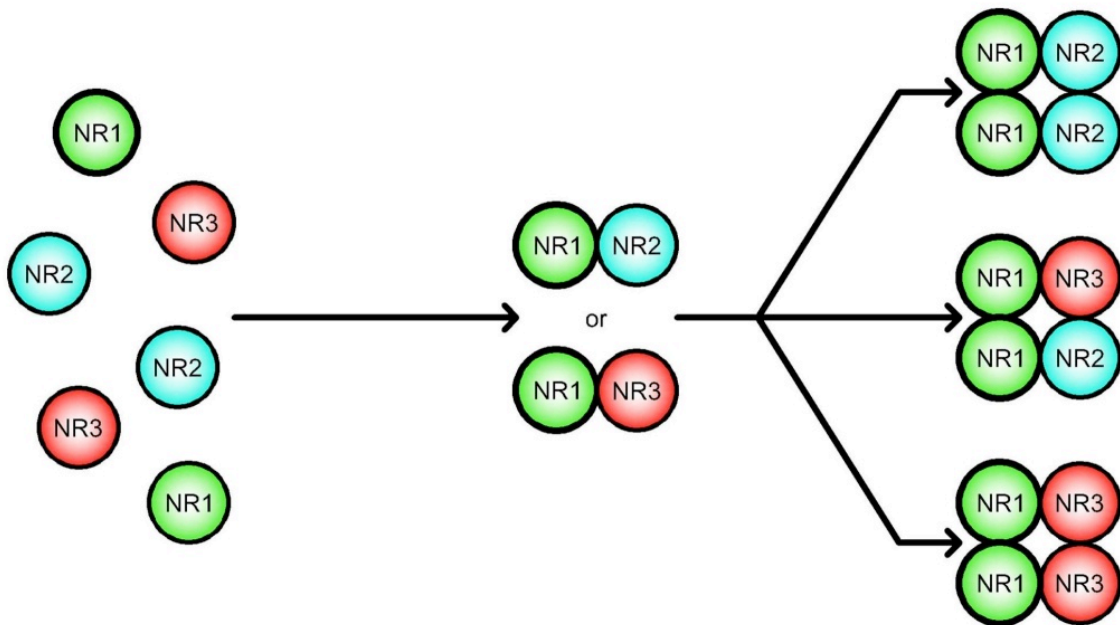


Figure 4. Formation of NMDA Receptors. NMDA Receptors form in a two-part process. The first step involves the association of an NR1 subunit with either an NR2 or NR3 subunit. In the next step two heterodimers of either NR1-NR2 or NR1-NR3 dimerize to form functional NMDA receptors. The two NR1 subunits hold the complex together through a disulfide bridge.

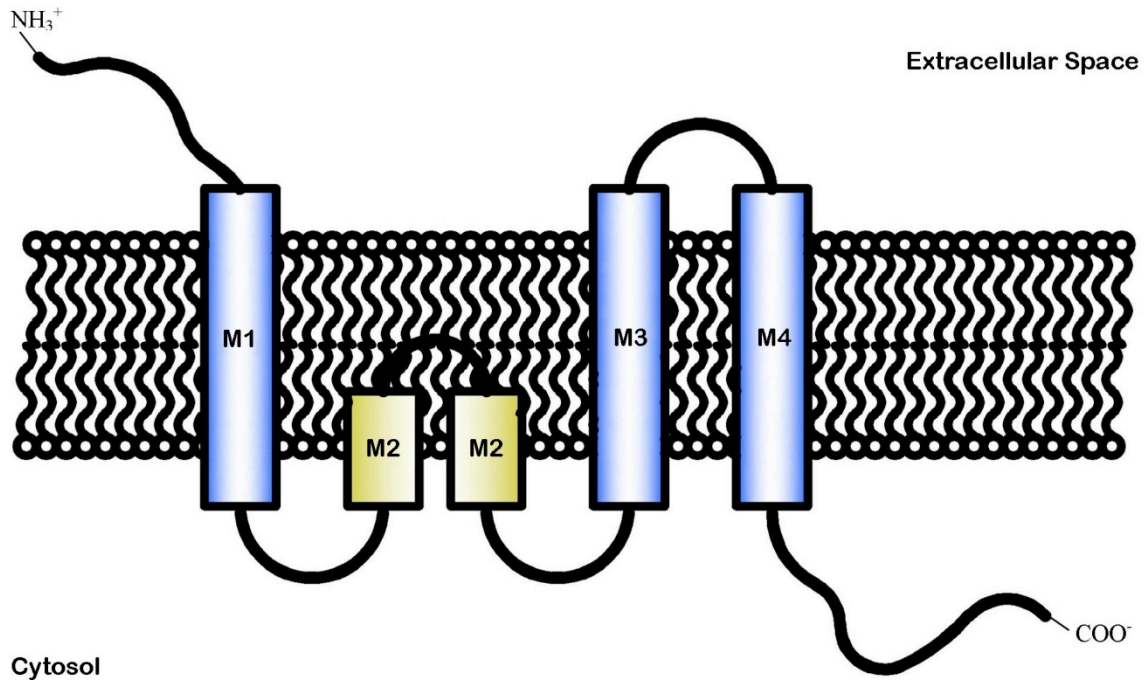


Figure 5. Membrane Domains of NMDA Receptors. NMDA Receptors subunits are typified by four transmembrane domains denoted at M1, M2, M3, and M4. M1, M3 and M4 span the phospholipid bilayer. M2 is a reentrant loop that is principally involved in forming the channel in NMDARs. The N-Terminal region of NMDARs is exposed to the extracellular space of cells while the C-terminal domain is found in the cytosol.

1.5 Non-Neuronal Distribution of NMDA Receptors

There is substantial evidence that NMDA receptors are expressed in non-neuronal tissues including heart (Gao et al., 2007; Morhenn et al., 1994; Seeber et al., 2000), kidney (Leung et al., 2004), pancreas (Inagaki et al., 1995), stomach (Covasa et al., 2000) skeletal tissue (Hinoi et al., 2003; McNearney et al., 2010), astrocytes (Krebs et al., 2003; Lalo et al., 2006) and oligodendrocytes (Karadottir et al., 2005).

These extraneural NMDARs play widely different roles compared to their neuronal counterparts. Work in rats showed that stomach NMDARs inhibit

histamine-induced reduction in mucosal blood flow (Tsai et al., 2004). In cardiac tissue, NMDARs may have a role in maintaining heart excitation and rhythm (Gill et al., 2007), though more recent work has also shown that over activation of these receptors may also have deleterious effects. Activation of these same NMDARs may lead to an increase in oxidative stress of cardiomyocytes and calcium load of cardiac mitochondria, which can ultimately lead to cell death (Tyagi et al., 2009). Alternate roles for NMDARs can also be seen in the kidneys where renal NMDARs control blood flow (Deng et al., 2002) and glomerular filtration rate (Deng and Thomson, 2009).

The expression of endothelial NMDARs has also been reported by many investigators (Betzen et al., 2009; Krizbai et al., 1998; Scott et al., 2007; Sharp et al., 2003; Sharp et al., 2005). Conspicuously, however, several groups were unable to confirm these results (Domoki et al., 2008; Morley et al., 1998; Preston et al., 1998). Therefore, the existence and function of endothelial NMDARS is an area of debate. Our laboratory has immunological evidence for endothelial NR1 and NR2C in culture and *in situ*. This fuels our interest in further understanding the link between endothelial NMDARs and brain vasodilation.

1.6 Nitric Oxide and Nitric Oxide Synthase

One of the most important molecules involved in vascular tone and blood flow regulation is NO. NO is a small gaseous organic molecule that easily diffuses across membranes to its site of action. NO is produced in many different cell types from a family of isoenzymes known as nitric oxide synthases (NOS). There are three known NOS enzymes: endothelial NOS (eNOS or NOS III), neuronal NOS (nNOS or NOS I) and inducible NOS (iNOS or NOS II). eNOS and nNOS constitutively produce low levels of NO in their resting state while iNOS must be activated to produce high levels of NO.

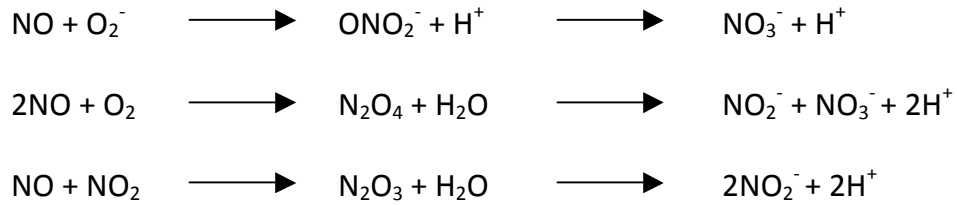
NOS is a complex enzyme that requires five additional co-factors to be functional. These co-factors are NADPH, heme, tetrahydrobiopterin, flavin adenine dinucleotide and flavin mononucleotide. The calcium binding protein calmodulin regulates NOS activity. Increases in intracellular calcium ions bind to calmodulin, which then undergoes a conformational change allowing binding to inactive NOS.

Active NOS catalyzes the formation of NO and L-citrulline from molecular oxygen and L-arginine. Many NOS inhibitors are either L-arginine analogues or urea/guanidine derivatives, which have differing affinities for the various NOS enzymes. NOS inhibitors that display no specificity for NOS subtypes include N^G-nitro-L-arginine (L-NNA), N^G-monomethyl-L-arginine (L-NMMA) and N^G,N^G-dimethyl-L-arginine (ADMA; Knowles and Moncada, 1994). Other Inhibitors

display specificity for particular NOS isozymes such as *N*-(3-(Aminomethyl)benzyl)acetamidine, more commonly known as 1400W. 1400W exhibits binding affinity to iNOS 5000-fold larger than that of eNOS and 250-fold greater than nNOS (Garvey et al., 1997). Relatively specific inhibitors for eNOS and nNOS include L-N(5)-(1-iminoethyl)ornithine (L-NIO) and 7-nitroindazole (7-NI) respectively.

NO is a potent vasodilator that relaxes vascular smooth muscle both *in vitro* and *in vivo*. Released NO activates soluble guanylate cyclase creating 3',5'-cyclic guanosine monophosphate (cGMP). This increase in intracellular cGMP activates protein kinase G which ultimately leads to inactivation of myosin light-chain kinase. The net result is dephosphorylation of the myosin light-chain and relaxation of smooth muscle cells (Surks, 2007). NO generated by macrophages and neutrophils is also released into invading microorganism as part of the immune response (Li et al., 2006; Nguyen et al., 1992; Wink et al., 1991).

NO is a small radical compound that is highly reactive as a result of an unpaired electron in its outermost orbital. Though NO has a relatively short half-life with a $t_{1/2}$ of approximately 5 seconds (Archer, 1993; Nathan, 1992) it may react with numerous other biomolecules to form nitrate (NO_3^-) and nitrite (NO_2^-). Some of the reactions that are known to occur *in vivo* include:



Most notable, NO may react with superoxide anion. This reaction results in the formation of peroxynitrite, a powerful oxidant that may have cytotoxic effects, which are not limited to DNA damage (Burney et al., 1999; Krizbai et al., 1998; Salgo et al., 1995) and damaging protein nitrosylation (Green et al., 1982; Viner et al., 1999).

Protein nitrosylation involvement in cell signaling has received attention in recent years. It has been shown that exogenous NO is able to nitrosylate cysteine residues to form nitrosothiols or tyrosine residues to produce N-nitrotyrosine (Mayer et al., 1998; Stamler et al., 1992; Stamler et al., 1997). Modification of cysteineyl groups in this way has been implicated in the regulation of many biological pathways through direct interactions such as S-nitrosylated mediated deactivation of NOS (Patel et al., 1996; Ravi et al., 2004), and dimethylarginine dimethylaminohydrolases (Leiper et al., 2002), enzymes involved in the conversion of arginine to NO. Another noteworthy effect of S-nitrosylation is inhibition of NMDAR function. *In vitro* experiments have shown that S-nitrosylation of heteromers consisting of NR1 and NR2A display a marked reduction in calcium influx upon nitrosylation of a single cysteine residue at position 339 (Choi et al., 2000; Lipton et al., 1993). Further

experiments have confirmed that NR2A is an endogenous substrate for NO-mediated nitrosylation (Lipton et al., 2002) and may be involved in the allosteric regulation of ligand binding (Hess et al., 2005).

1.7 Implications of Neurovascular Dysfunction in Dementia

Dementia is a neurological disease characterized by cognitive impairment. Vascular dementia and Alzheimer's disease (AD) are the two most common forms of cognitive impairment in the elderly (Fotuhi et al., 2009) and while these two diseases have been considered separate for many years, emerging evidence suggests that the pathogenesis of both diseases is routed in cerebrovascular dysfunction (Iadecola, 2010)

In addition to being a disease typified by neurodegeneration, AD has a strong vascular component. As AD progresses, profound changes in cerebrovascular structure and function have been observed. In regards to structure, microvessel numbers are reduced, endothelial cells adopt a more flattened conformation and smooth muscles cells of the cerebrovasculature become degenerated (Kalaria, 1997). Functional changes such as reduced cerebral blood flow at rest and impairment in functional hyperemia also become apparent. These changes are hypothesized to occur in response to the accumulation of A β . Mouse models of AD where amyloid precursor protein is overexpressed to promote the formation of A β have demonstrated a marked

inability to regulate cerebral blood flow (Iadecola, 2004). CBF dysfunction can be reproduced in healthy normal mice by topical superfusion of $A\beta_{1-40}$ to the neocortex (Niwa et al., 2000; Park et al., 2004). Plaque formation alone is unable to explain the cognitive impairment and decline of patients as some patients have the aforementioned clinical signs of AD but no $A\beta$ plaques (Gomez-Rodriguez et al., 2008). $A\beta$ can occur either as a soluble peptide that acts as a powerful vasoconstrictor or an insoluble aggregate that forms polymers, which is responsible for plaque and tangle formation. Disruption of blood flow reduces clearance of $A\beta$ from the brain leading to its accumulation in cerebral blood vessels. This process of growing $A\beta$ aggregates is known as cerebral amyloid angiopathy and has been found to be associated with cognitive decline. Other studies have shown that as the disease progresses resting blood flow decreases and functional hyperemia is attenuated (Agbaje et al., 2008; Mentis et al., 1996; Warkentin and Passant, 1997).

Free radical generation plays a key role in cerebrovascular dysfunction. Loss of blood flow regulation leads to local regions of hypoxia and ischemia in the brain, which damages neural white matter contributing to the cognitive decline observed in dementia patients (Iadecola, 2010). Oxidative stress and free radical generation can also trigger inflammatory responses in the cerebrovasculature. Inflammation further exacerbates the generation of

radical oxygen species by increasing expression of radical generating enzymes while reducing cellular antioxidant defense mechanisms (Gill et al., 2010).

1.8 RATIONALE

While it is well established that neural activity is strongly coupled to the supply of nutrients and oxygen to active areas of the brain by activating astrocytes, the molecular basis for how this occurs is less well understood. There are several types of cells involved in this process that together make up the neurovascular unit (figure 6). These cells include neurons, astroglia, pericytes, smooth muscle cells and endothelial cells.

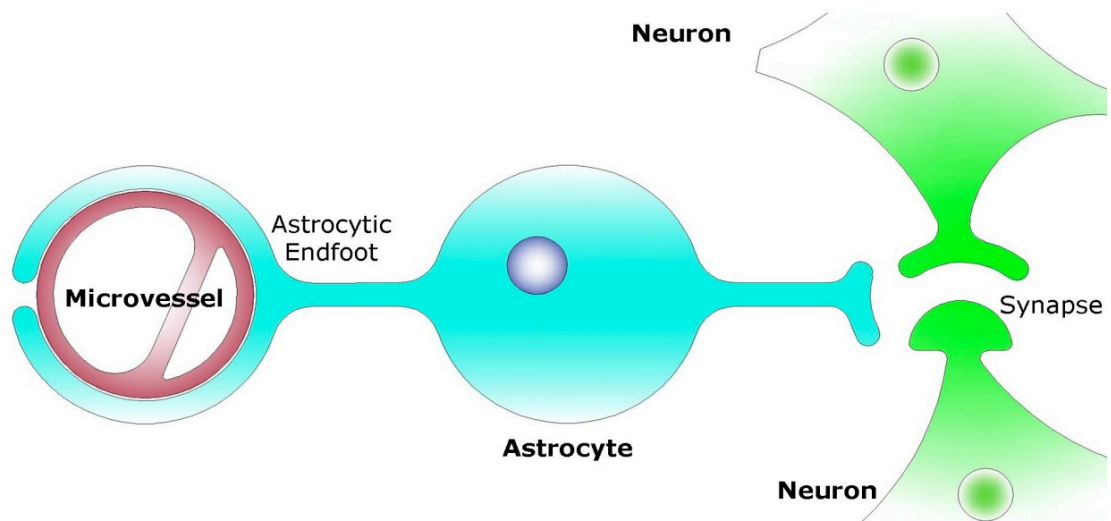


Figure 6. Schematic Representation of the Neurovascular Unit. The neurovascular unit is comprised of three main components: neurons, astrocytes and microvessels. Neural activity is sensed by neighboring astrocytes at neural synapses. Astrocytes respond to this increase in neural activity by releasing vasoactive compounds from endfeet, which ensheath nearby microvessels. Dilatation of vessels leads to an increase in local blood flow to supply oxygen and nutrients.

During neural activity the neurotransmitter glutamate is released across the synaptic cleft, which has two effects on neighboring cells related to functional hyperemia. Firstly, glutamate released can activate neuronal NMDA receptors triggering activation of nNOS and subsequent neuronal release of NO. As mentioned, this is a mechanism of functional hyperemia with significant support. Astrocytic processes located at the synapse also respond to glutamatergic transmission with an increase in intracellular Ca^{2+} , including in astrocytic endfeet surrounding nearby blood vessels. The focal increase in calcium at endfeet promotes the secretion of vasoactive substances to nearby vessels thereby causing vasodilation or relaxation of the vessels. Proposed substances responsible for the observed dilatory effects of action include ADP, potassium and products of arachidonic acid metabolism (Vanhoutte and Mombouli, 1996).

We have evidence of another astrocyte-mediated mechanism that implicates endothelial NMDA receptors and eNOS. When precontracted middle cerebral arteries removed from male mice are treated with the NMDA receptor agonists glutamate and D-serine the vessels relax. Coexposure of these vessels with NMDA receptor antagonists specific for the glutamate and D-serine binding sites attenuated this dilatory response while the AMPA/kainate receptor antagonist had no effect. The dilatory response to NMDA receptor agonists suggests that the observed vessel relaxation is NMDA

mediated and occurs at the level of the vessel. Blockade of these responses by eNOS inhibitors and removal of the endothelial cell layer of vessels suggest that endothelial NMDA receptors are responsible. Since astrocytes are capable of secreting D-serine in response to calcium transients our lab postulates that astrocytes release D-serine, which can act at endothelial NMDA receptors causing vasodilation. Recent work in brain slices from our lab by Jillian LeMaistre support this by showing that vasodilation in response to increase in calcium in astrocytes is dependent on D-serine release.

1.9 HYPOTHESIS AND OBJECTIVES

The specific hypothesis for this project examines part of this postulate, which is that **activation of endothelial NMDA receptors leads to an increase in intracellular calcium levels activating endothelial nitric oxide synthase to produce the vasodilator nitric oxide.**

We tested our hypothesis using an immortalized mouse brain endothelial cell line, bEnd.3. The success of other groups examining putative NMDA receptors in the same cell line and favorable reports of retention of endothelial blood brain barrier characteristics were behind the decision to use this model (Betzen et al., 2009; Scott et al., 2007). The objectives of my experiments were; 1) determine whether bEnd.3 cells expressed functional NMDARs; 2) elucidate the NMDAR subunits expressed in bEnd.3 cells and; 3) show that exposure of

bEnd.3 cells to solutions of the NMDAR agonists and coagonists glutamate and D-serine precipitated an increase in NO production.

MATERIALS AND METHODS

2.1 Culture of bEnd.3 Cells

The immortalized mouse brain endothelial cell line bEnd.3 was maintained and used in experiments for up to 20 passages. bEnd.3 cells were cultured in Dulbecco's modified Eagle's medium (DMEM) supplemented with 2 mM L-glutamine, 10% fetal bovine serum (FBS) and 0.02% streptomycin. Cells were grown to 85-95% confluence at 37°C and 5% CO₂, at which point they were passaged. Passaged cells were washed twice with Phosphate Buffered Saline (PBS) solution (10 mM PO₄²⁻, 2.7 mM KCl, 137 mM NaCl, pH 7.4) prior to treatment with 0.25% trypsin-EDTA (2-[2-(Bis(carboxymethyl)amino)ethyl-(carboxymethyl)amino]acetic acid) for 8 minutes at 37°C. Trypsin activity was subsequently deactivated by addition of 8000 µL DMEM.

Cells were seeded in 75 cm² flasks at a density of 1.3x10⁴ cells/cm². 10cm dishes, 6-well dishes and 96-well plates were plated at densities of 6.4x10² cells/cm².

2.2 Preparation of Protein Extracts

bEnd.3 cells were grown to confluence in 6-well plates and placed on ice. Lysis of cells was accomplished by addition of 200 µL Laemlli Buffer (50 mM Tris(tris(hydroxymethyl)aminomethane), 2% sodium dodecyl sulfate (SDS), pH 6.8) and protease inhibitor cocktail (Roche, Mini Complete tablets, 1

tablet/mL). Cells were lysed directly in wells and the resulting lysate transferred to 1.5 mL Eppendorf tubes. Lysate was triturated with a 20.5 GA needle to shear genomic DNA, reducing viscosity. Protein concentrations were measured using the Bradford Assay (Bradford, 1976). Protein samples were either used the same day or aliquoted into 1 mL Eppendorf tubes and stored at -20°C.

A similar protocol was used for protein extractions from mouse brain tissue. Approximately 5 volumes of Laemlli buffer was added to brain tissue extracted from 15 week old CD46 mice and ground with an electric pestle. Samples were then spun for 15 minutes at 12000 x *g*, pelleting cellular debris. Lysate was decanted from the pellet and spun for an additional 10 minutes to minimize contamination from insoluble cellular debris. Measurement of protein concentration and storage was identical to methods used for cultured cells.

2.3 Western Blotting

Proteins from whole cell lysates were separated on 7.5%, 1.5 mm SDS-PAGE gels using a constant voltage of 80 V through the stacking gel and 120 V through the running gel. Transfer of proteins to a microporous polyvinylidene difluoride (PVDF) membrane was done by electro blotting. Proteins were transferred from the gel to the PVDF membrane in transfer buffer (25 mM

Tris, 192 mM glycine, 10% methanol, pH 8.0) at 220 mA for 1 hour at 4°C. Membranes were next blocked in Tris-buffered saline solution (20 mM Tris-HCl, pH7.5 150 mM NaCl) with 0.1% Tween-20 (TBST) and 5% non-fat skim milk for 8 hours at 4°C before incubation in a primary antibody solution containing 5% non-fat skim milk and 1% bovine serum albumin (BSA) in TBST. Primary antibody applications (see Table 2 for a complete list of antibodies) were incubated overnight at 4°C on a rocker. Membranes were subsequently washed 5 times for periods of 5 minutes in TBST to remove excess primary antibody before incubation with the appropriate secondary HRP-linked (horse radish peroxidase) antibody (table 2). Membranes were incubated with secondary antibody for 1 h at room temperature.

Table 2. Antibodies used in Western Blot Probing

Antibody	Company	Catalogue Number	Isotype	Epitope (Species)
NR1	Chemicon	MAB363	mouse IgG	660-811 (na)
	EMD	454578	mouse IgG	(na)
	Sigma	G8913	rabbit IgG	918-938 (r)
	Sigma	M-207	rat IgG	(na)
NR2A	Chemicon	AB1555P	rabbit IgG	1253-1391 (r)
NR2B	Chemicon	AB1557P	rabbit IgG	C-terminus (m)
NR2C	Santa Cruz Biotechnology, Inc	sc-1470	goat IgG	C-terminus (na)
	Santa Cruz Biotechnology, Inc	sc-31547	goat IgG	N-terminus (h)
	Santa Cruz Biotechnology, Inc	sc-50437	rabbit IgG	21-100 (h)
NR2D	Santa Cruz Biotechnology, Inc	sc-10727	rabbit IgG	268-386 (h)
NR3A	Upstate	07-356	rabbit IgG	1098-1113 (r)
NR3B	Upstate	07-351	rabbit IgG	916-930 (m)
Goat IgG	Santa Cruz Biotechnology, Inc	sc-2020	donkey IgG	(na)
Rabbit IgG	Cell Signalling	7074	mouse IgG	(na)

h, human; m, mouse; r, rat; na, information not available.

After incubation membranes were washed an additional 5 times for 5 minutes in TBST. Following washing, membranes were covered with a chemiluminescent reagent (ECL Plus, Amersham) for 15 minutes in low light conditions after which ECL reagent was removed by pipette. Images were captured using a Fluor-S Max Multimager (Bio-Rad) with 55 mm, f1.4 lens (Canon). Resulting pictures were processed using Quantity One (Bio-Rad).

2.4 Calcium Imaging

bEnd.3 cells were grown to confluence in 6-well plates on 25 mm glass cover slips (Electron Microscopy Sciences). Media was aspirated from wells and cells incubated in Locke's Buffer (154 mM NaCl, 3.6 mM NaHCO₃, 5.6 mM KCl, 1.0 mM MgCl₂, 5 mM glucose, 5 mM HEPES [N-2-Hydroxyethylpiperazine-N'-2-Ethanesulfonic Acid], 2.3 mM CaCl₂, pH 7.2) containing an additional 0.1% BSA and 5 μM FURA 2-AM (Fura-2-acetoxymethyl ester) for 45 minutes at 37°C and 5% CO₂. After incubation cells were washed twice for 10 minutes with Locke's buffer to remove traces of excess extracellular FURA-2. Cover slips were next placed in a cover slip holder in 500 μL Locke's buffer and viewed using an inverted research microscope (Olympus, IX71). Fluorescence intensity was measured at 500 nm using excitation wavelengths of 340 nm and 380 nm. Data was captured and analyzed using software by PTi (PTi, V.1.04). Cells were treated once baseline A340/380 ratios were consistent (deviated by not more

than ± 0.05). Cells were treated with 10 mM, 1 mM, 500 μ M, 100 μ M and 50 μ M glu \pm equal concentrations of D-ser. 10 mM ionomycin, 2 mM thapsigargin, 90 mM KCl and 100 μ M ACh were used as positive controls.

2.5 Polymerase Chain Reaction

Total RNA was purified using the RNeasy® Mini kit (Qiagen). For each extraction 10 μ L β -mercaptoethanol (β -ME) was added to 1 mL fresh lysis buffer (RLT buffer, Qiagen). RNA from bEnd.3 cells and whole tissue homogenates were collected using a different method. Total RNA from bEnd.3 cells was harvested through direct lysis of the cells in 10 cm dishes by addition of 500 μ L RLT buffer and scraped. Lysate was transferred to a 1 mL Eppendorf tube using a sterile 1 mL syringe and 20.5 GA needle, which was then triturated to break up cellular debris. Total RNA from tissue extracts, was performed by adding \sim 30 mg of tissue to an Eppendorf along with 600 μ L RLT buffer. Tissue was next homogenized by grinding with a motorized pestle for 30-40s. Following homogenization lysate was triturated using a 1 mL syringe and 20.5 GA needle. Lysate was centrifuged for 3 minutes at 14000 rpm to pellet any insoluble debris with subsequent decanting of the lysate to a new clean Eppendorf tube. Total RNA was isolated from cleared lysates in both types of purification methods as detailed by the manufacturer's instructions. Final

concentration of RNA was determined by reading absorbance at 260 nm and 280 nm and using the 260:280 ratios as an index for purity.

Total RNA was converted to cDNA using iScript™ cDNA Synthesis kit (Bio-Rad) following the instructions provided by the manufacturer. In each instance 500 ng RNA template was used per 20 µL reaction. The resultant cDNA was used in subsequent polymerase chain reaction (PCR) amplification experiments.

Amplification was carried out following the protocol provided by Invitrogen. The final concentration of components for PCR reactions were 1X PCR Buffer (Invitrogen), 0.2 mM dNTP mixture (Invitrogen), 1.5 mM MgCl₂, 0.2 µM left primer, 0.2 µM right primer, 1.0 units Platinum® *Taq* DNA polymerase (Invitrogen) and DNA template. Reactions were made to a final volume of 50 µL with sterile ddH₂O (Invitrogen). Reaction mixtures were incubated in an iCycler (Bio-Rad) thermal cycler using the cycles shown in Table 3.

Table 3. Cycle number, temperatures and times used in PCR amplification of cDNA.

Step	Cycles	Temperature (°C)	Time (min:sec)
1	1	94	2:00
2	30	94	0:30
		62.5	0:30
		72	0:20
3	1	72	7:00
4	1	4	∞

PCR product was run on a 2% agarose gel stained with ethidium bromide (0.5 $\mu\text{g}/\text{mL}$). 7 μL from each sample was loaded into a lane and a constant voltage of 120 V was applied for 25-35 minutes. Images of visualized bands were acquired using a Gel Doc XR imager and processed using Quantity One (Bio-Rad).

Primer sequences for PCR experiments were designed using software from Primer 1 (Table 4). mRNA primers for the various NMDARs were synthesized by InvitrogenLife Technologies. PCR product amplified from bEnd.3 cells was sequenced by University Core DNA Services at the University of Calgary.

Subunit	Forward Primer	Reverse Primer	NCBI Ref ID	Forw Ref #	Rev Ref #	Product
NR1	GCTGTACTGCTGGACCGCT	GATCATCGTGGCTTCTTACTGCTGC	ref NM_008169.1 	1821-1840	2016-2039	219
NR2A	AAGCCCCCTTTCATCGTA	CAAGGGGTTCTGCATGACA	ref NM_008170.2 	365-384	519-538	174
NR2B	GCTACAACACCCACGAGAAGAG	GGAAAAGTGTGGACCCCTCTC	ref NM_008171.3 	1725-1746	2020-2038	314
NR2C	AACCAACCTTCAGCAGCG	CTCACCAAAGGCAAGAAAGTC	ref NM_010350.2 	2085-2103	2529-2548	464
NR2D	CGATGGGCTGGAAATGG	CGCCGTCACAGTTTTCATCT	ref NM_008172.2 	1656-1673	1896-1915	261
NR3A	CCCTCCCAACTCTCCGTTGA	TCGTGCTGCTGTGCATAGGA	ref NM_001033351.1 	1631-1650	1804-1823	193
NR3B	CCCAAGCTCAACGCTTCAT	CCTTTGGGATGGAGGGCTTAC	NM_130455.3	2385-2404	2476-2495	111

Table 4. PCR Primer Sequences. Forward and reverse primer sequences used in the amplification of NMDAR subunit mRNA. NCBI Ref ID is the sequence ID from which the primers were designed. Forw Ref # and Rev Ref # are the base pair numbers that the primers correspond to. Predicted product size is given in base pairs.

2.6 Nitric Oxide Assay

bEnd.3 cells were grown to confluence in 6-well plates. Once confluent, cells were treated for a period of 24 or 48 hours in 2 mL solutions of DMEM supplemented with either 100 μ M-10 mM glutamate, or a combination of 1 μ M-1 mM D-serine and glutamate. A 1 mM solution of Ach was used for a positive control. NO production was measured indirectly by colorimetric analysis of nitrite concentration based on the Griess reaction (Green et al., 1982). At each time point plates were gently swirled by hand and 100 μ L media from each sample was dispensed into one well of a 96-well plate. To each sample was added 50 μ L 1% sulfanilamide in 5% phosphoric acid followed immediately by the addition of 50 μ L N-(1-Naphthyl)ethylenediamine dihydrochloride. Color was allowed to develop for each plate at room temperature in the absence of light for 15 minutes. After 15 minutes the optical density of each well was measured at 540 nm (FLUOstar Omega; BMG Labtech) Concentration of nitrite was quantitated by comparing against a standard curve of calcium nitrite (Cayman Chemical, Sigma-Aldrich) with concentrations from 0-15 μ M in 5 μ M increments. Nitrite standard solutions were treated identically to those used in the bEnd.3 media preparations.

2.7 Slot Blotting

bEnd.3 cell lysates were extracted and purified as detailed above. Cell extracts were used the same day. To set up apparatus two sheets of blotter paper (GB002, Whatman) and a nitrocellulose membrane were pre-wet in PBS for 15 minutes. Membranes and paper were placed on vacuum manifold and vacuum was applied constantly. Wells were washed with 100 μ L PBS prior to sample loading. 10 μ g protein solutions were made in 250-300 μ L PBS and boiled at 100⁰C for 10 minutes prior to loading onto slot blot membrane. After loading each well was washed twice with an additional 100 μ L PBS. Following washing vacuum pressure was removed and the membrane was placed in a blocking solution comprised of Tris-buffered saline solution, 0.1% Tween-20 (TBST) with 5% non-fat skim milk. Next, membranes were incubated in blocking solution with a 1:600 dilution of rabbit anti-mouse anti-nitrotyrosine antibody (Millipore, 06-284) overnight on a rocker at 4⁰C. Membranes were subsequently washed the next day 5 times for periods of 5 minutes in TBST to remove excess primary antibody before incubation with a secondary HRP-linked antibody. Membranes were incubated with secondary antibody for 1 h at room temperature. Membranes were washed an additional 5 times for 5 minutes in TBST. Following washing, membrane was covered with chemiluminescent reagent (ECL Plus, Amersham) for 15 minutes in low light conditions before clearing excess liquid with a pipette and imaged. Images

were captured using a Fluor-S Max Multimager (Bio-Rad) with 55 mm, f1.4 lens (Canon). Resulting pictures were processed using Quantity One (Bio-Rad). Densitometric analysis was carried out using ImageJ software.

2.8 Statistical Analysis

All statistical analysis was done using Graphpad Prism® version 4.02 software program (Graphpad software, San Diego, CA). Both the Student's *t*-test and 1-way ANOVA analyses were used to evaluate statistical comparisons. Differences were considered to be significant if $p < 0.05$. Data are presented as mean \pm S.E.M. Student Newman-Keuls post-tests were performed on all 1-way ANOVA analyses except for dose response analysis, for which a Dunnett's test was performed, comparing all columns to the control.

RESULTS

3.1 bEnd.3 Cells Transcribe mRNA for NMDAR Subunits

RT-PCR amplification was employed for detecting the mRNA of the seven known NMDAR subunits in the bEnd.3 cell line. We showed that bEnd.3 cells transcribe mRNA for the NR1, NR2B, NR2C, NR2D and NR3B subunits. No PCR product was detected for the NR2A and NR3A subunits (figure 7A). RT-PCR was performed on RNA samples extracted from whole mouse brain as a positive control for each unit subtype. mRNA for all NMDAR subunits was found in mouse brain (figure 7B).

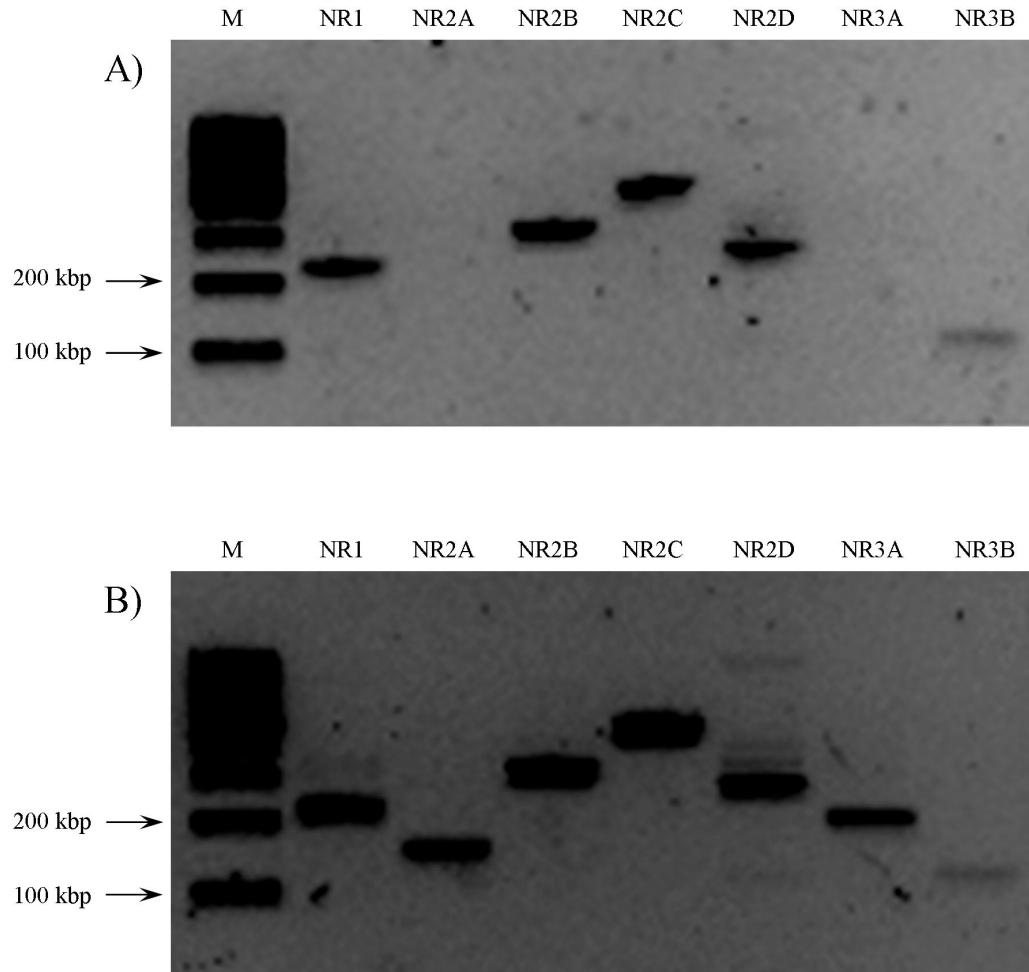


Figure 7: PCR amplification of NMDARs in bEnd3 cells and whole mouse brain. 10 μ g of RT transformed RNA extracted from either bEnd3 cells (A) or whole mouse brain tissue (B) were loaded onto a 2% agarose gel and run at a constant voltage of 120V for 20 minutes. Lanes were, from left to right, 100 bp marker (M); NR1 with expected size of 219 bp; NR2A with expected size of 150 bp; NR2B with expected size of 314 bp; NR2C with expected size of 464 bp; NR2D with expected size of 193 bp; NR3A with expected size of 193 bp and; NR3B with expected size of 111 bp.

3.2 bEnd.3 Cells Express NMDAR NR1 and Other Subunits

Using Western blotting, an immunoreactive product consistent with the expected 115 kDa band for NR1 was observed in bEnd.3 cell, cortical and cerebellar homogenates (figure 8A). Similarly, the expected 130 kDa band was

observed for NR2C (figure 8B). No immunoreactive bands were observed at or near the expected size in bEnd.3 homogenates for NR2B or NR2D despite evidence for the expected bands in brain control lanes (figure 8C and D). For NR2A, NR3A and NR3B immunoreactive products were observed in the general size range of the expected band size. In each case these bands differed from the expected band size by more than 10 kDa, making interpretation difficult (figure 8E, F and G).

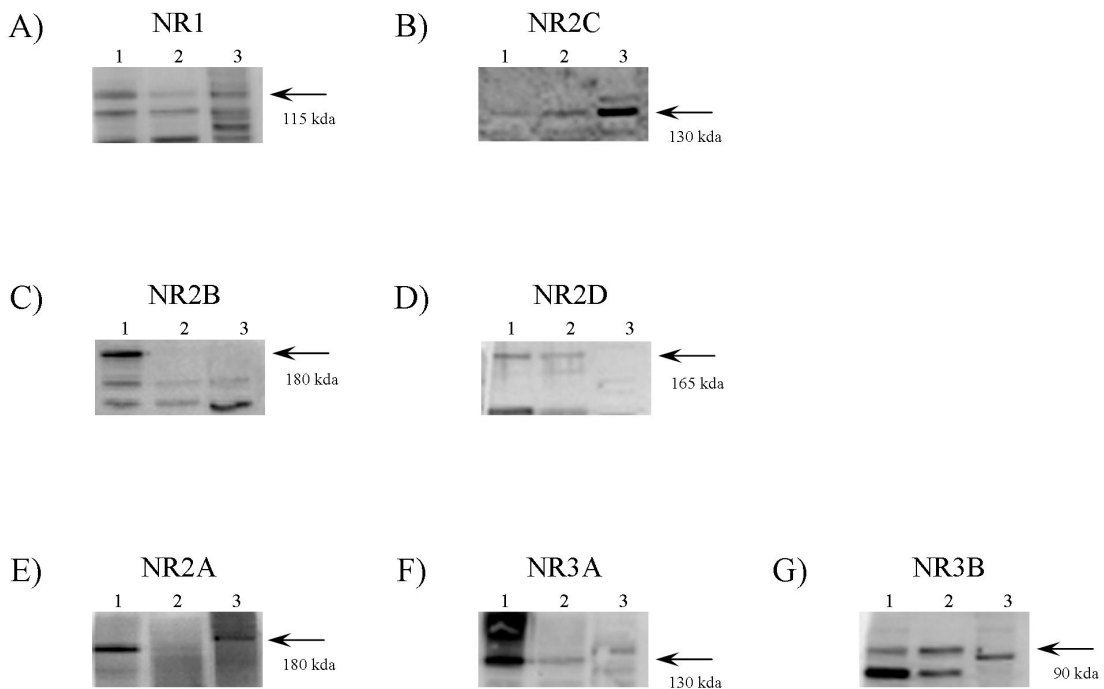
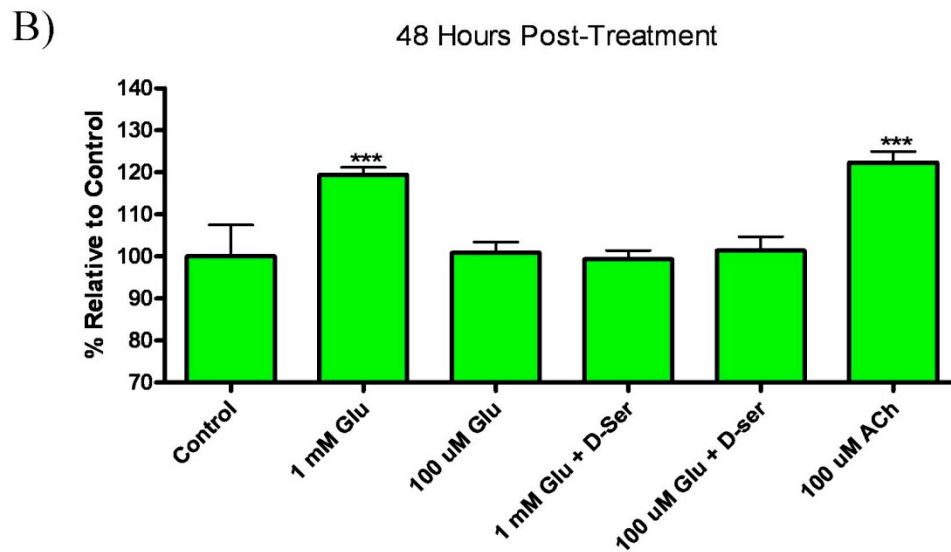
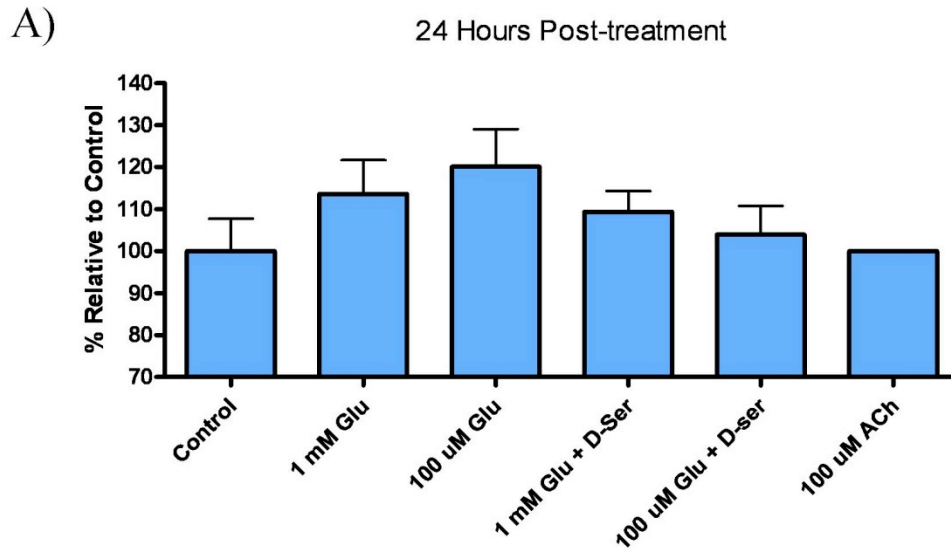


Figure 8. Western Blot Probing of NMDARs. The presence of NMDA receptor subunits 1 (A) and 2C (B), in 20 µg protein extracted from bEnd.3 cells (lane 3). No evidence for receptor subunits NR2B (C) and NR2D (D). Results for probing of protein extracts with antibodies against NR2A (E), NR3A (F) and NR3B (G) uninterpretable. Antibodies used were also tested against 20 µg cerebellar (lane 1) and 20 µg cortical (lane 2) tissue extract.

3.3 Treatment of bEnd.3 Cells with Glutamate and D-Serine Causes no Significant Increase in Nitrite Production

In primary endothelial cells, exposure to ACh results in the release of NO. We expect activation of endothelial NMDARs to release NO in response to glutamate and D-serine exposure and that the magnitude of this release should resemble that of stimulated ACh receptors. To test whether activation of the endothelial NMDARs would produce a similar increase in NO production we used the Griess method. The Griess method was used to test for production of NO by measuring changes in nitrite production following glutamate and D-serine exposure. Treating bEnd.3 cells with glutamate with and without D-serine produced no significant changes in total nitrite at 24 hours of continuous exposure (figure 9). The same trend was observed after 48 hours of agonist exposure, with the notable exception of 1 mM glutamate ($p < 0.001$). Nitrite production using 100 μ M ACh yielded a significant increase in observed nitrite production after 48 hours ($p < 0.001$), serving as a positive control and indicating that glutamate and D-serine do not produce NO levels comparable to ACh.

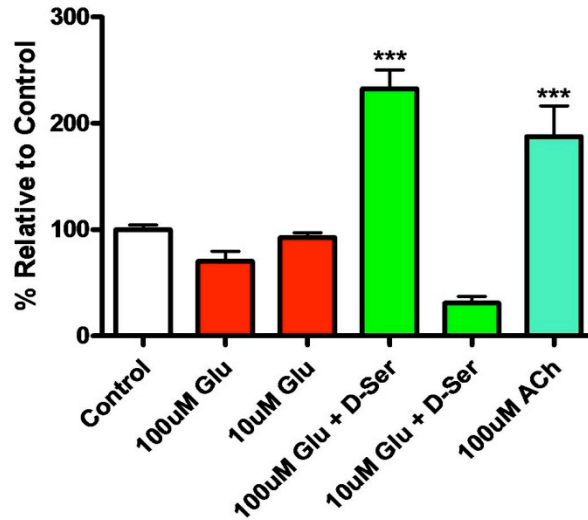


*** : $p < 0.001$

Figure 9: Nitrite Concentration in DMEM 24 and 48 Hours Post-Treatment of Confluent bEnd3 Cells with Glutamate or Combination of Glutamate and D-Serine. bEnd3 cells were grown to confluence in 6-well plates. Once confluent cells were treated with either 1 mM or 100 μM glu else treatment with a combination of glu and D-ser at concentrations of 1 mM or 100 μM in fresh DMEM. Concentration of nitrite expressed as a percentage relative to that observed in a control sample with no glu or D-ser treatment. A) At 24 hours there is no significant difference between nitrite produced in control and treatments groups. B) At 48 hours a significant difference in nitrite production observed for 1 mM glu treatment and 100 μM ACh ($p < 0.001$) when compared to the control. No significant difference is recorded with other treatment groups.

3.4 Treatment with Glutamate and D-Serine Causes an Increase in S-Nitrosylated Protein Dependent on NMDAR Activity

To gain further insight into NMDA receptor mediated production of NO, we measured nitrosylated tyrosine residues by slot blot of total cell lysates as a downstream indicator of NO-mediated nitrosylative stress. Incubation of bEnd.3 cells for 24 hours with glutamate alone caused no significant change in S-nitrosylated protein using concentrations of glutamate between 100 μ M and 10 μ M (figure 10). In contrast to the nitrite results, when cells were treated with glutamate and D-serine, a significant increase in S-nitrosylated protein was seen following dosing and 24 hour incubation with 100 μ M glutamate and D-serine ($p < 0.001$). No significant increase was found at 10 μ M glutamate and D-serine. A 100 μ M treatment with ACh as a positive control (teal) also produced a statistically significant increase in nitrosylation, as expected.



*** : $p < 0.001$

Figure 10: Dose Response of Protein S-Nitrosylation in bEnd3 Cells with Glutamate \pm D-Serine. bEnd.3 cells were grown to confluence in 6-well plates. Once confluent cells were treated with either 100 μ M, or 10 μ M glu \pm D-ser in fresh DMEM for 24 hours before harvesting. S-nitrosylated proteins were determined by slot-blotting and band intensity analyzed using densitometry. Significance was determined by comparing groups to a control with no glu or D-ser. 100 μ M ACh was used as a positive control.

We next tested whether the increase in nitrosylated protein was dependent on NMDAR activation. Protein nitrosylation was significantly higher in groups treated with 100 μ M glutamate and D-serine alone ($p < 0.001$; figure 11). bEnd.3 cells were then treated with 100 μ M glutamate and D-serine with and without either 20 μ M NMDAR glycine site antagonist DCKA or 50 μ M NMDAR glutamate antagonist AP5. Vehicle controls were used in all experiments involving DCKA (0.1% DMSO in DMEM). After treatment with DCKA we observed significant attenuation in protein nitrosylation relative to proteins extracted from the control group. The glutamate site antagonist AP5 also significantly reduced this effect (figure 11). To ensure that the observed increase in nitrosylated protein was not due to activation of endothelial

AMPA/kainate receptors we used the AMPA/kainate receptor antagonist, CNQX. 24 hours post continuous exposure to glutamate/D-serine, CNQX had no effect on protein nitrosylation. Vehicle controls were used in all experiments involving CNQX (0.1% DMSO in DMEM).

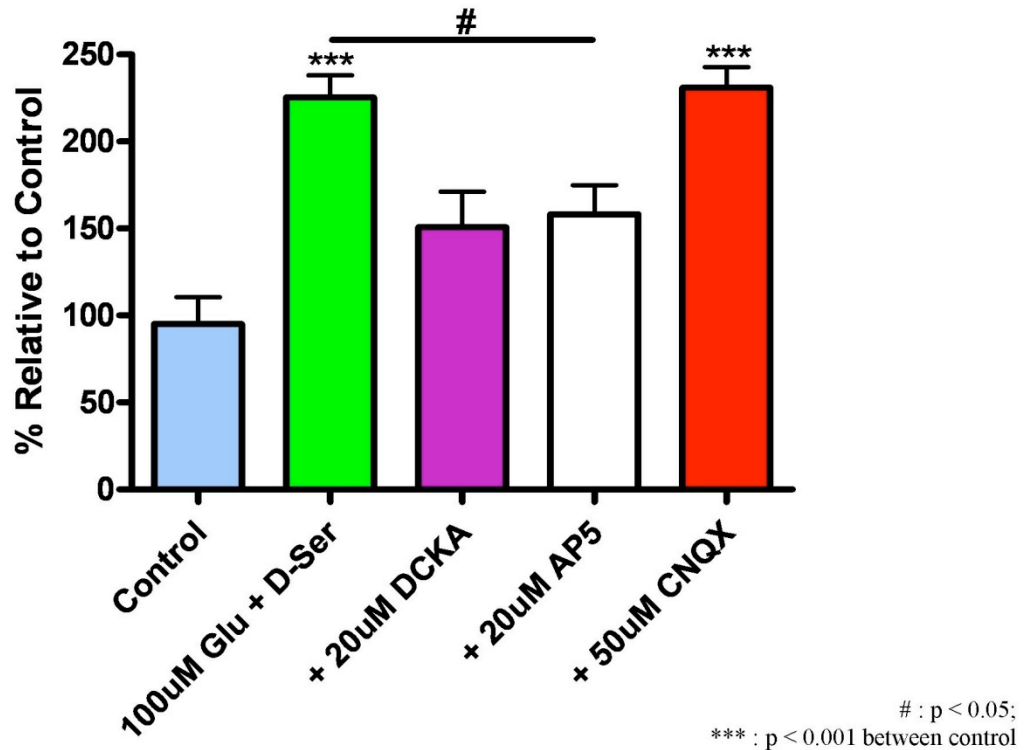
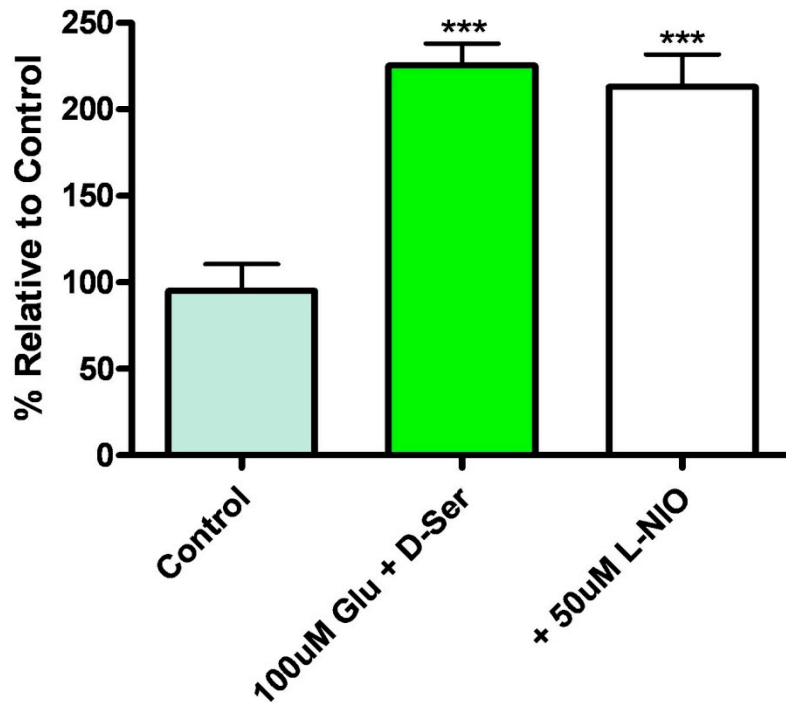


Figure 11: Protein S-Nitrosylation in bEnd3 Cells with Glutamate and D-serine ± Antagonists. bEnd3 cells were grown to confluence in 6-well plates. Once confluent cells were treated with either 100µM glu and D-ser for 24 hours with no NMDAR antagonist (green), 20 µM NMDAR glycine site antagonist DCKA (purple) 20µM NMDAR glutamate site antagonist AP5 (white) or 50 µM mGluR/kainate receptor antagonist CNQX. A significant rise in protein nitrosylation was observed in the lysate extracted from cells treated with glu and D-ser alone or those coexposed to 50 µM CNQX when compared to the untreated control group (p < 0.001). Treatment with NMDAR antagonist significantly reduced this effect when compared to NMDAR agonist treatment (p < 0.05).

3.5 S-Nitrosylation is Not eNOS-Related

Examining whether the increase in nitrosylated proteins was due to activation of eNOS, bEnd.3 cells were coexposed to 100 μ M NMDAR agonists glutamate and D-serine, and 50 μ M of the selective eNOS inhibitor L-NIO. Protein nitrosylation was not significantly different from the glutamate/D-serine treatments alone indicating that eNOS is not necessary for enhanced nitrosylation ($p < 0.001$; figure 12).



*** : $p < 0.001$

Figure 12: Protein S-Nitrosylation in bEnd3 Cells \pm eNOS Antagonist. bEnd3 cells were grown to confluence in 6-well plates. Once confluent cells were treated with either 100 μ M glu and D-ser for 24 hours with no NMDAR antagonist (green) or 50 μ M eNOS antagonist L-NIO (white). Significant nitrosylation of proteins was observed when comparing treatment groups to the control group ($p < 0.001$).

3.6 Glutamate and D-Serine Elicit Small Increases in Intracellular Calcium Levels

As NMDARs characteristically gate an influx of intracellular calcium we investigated whether activation of NMDARs in bEnd.3 cells produces increases in intracellular Ca^{2+} . Changes in intracellular calcium were monitored by ratiometric imaging of calcium using the fluorescent probe fura-2 am. After achieving a steady baseline cells were treated with positive controls. When cells were treated with the calcium ionophore, ionomycin (figure 13A), a significant increase in intracellular calcium levels was observed suggesting that extracellular calcium levels were sufficiently high to promote an increase in bEnd.3 cell calcium levels. Similarly thapsigargin triggered a rise in intracellular calcium indicating that we could measure calcium increases from intracellular sources. (figure 13B). In a third positive control, 90 mM KCl also triggered a transient rise in intracellular calcium that lasted almost 5 minutes before baseline calcium levels were reestablished (figure 13C) indicative of calcium channels activity.

In an extension of studies done in section 3.4, showing that glutamate and D-serine together produce an increase in protein nitrosylation, bEnd.3 cells were treated with a combination D-serine and glutamate and the rise in intracellular calcium monitored. ACh was used as a comparator because it is a known activator of calcium levels and eNOS in endothelial cells. After

treatment with 100 μ M of both NMDAR agonists an increase in the A340/380 ratio was recorded, indicating a significant increase in intracellular calcium. Following NMDAR coagonist treatments cells were treated with 100 μ M ACh, which produced an increase in intracellular calcium levels of a larger magnitude. ACh and glutamate/D-serine induced calcium responses are summarized in figure 14B. ACh produced a 2-fold increase in calcium over baseline ($p < 0.001$, $n=14$). The effect of glutamate and D-serine was 1.7-fold smaller than ACh but was statistically significant ($p < 0.001$, $n=14$).

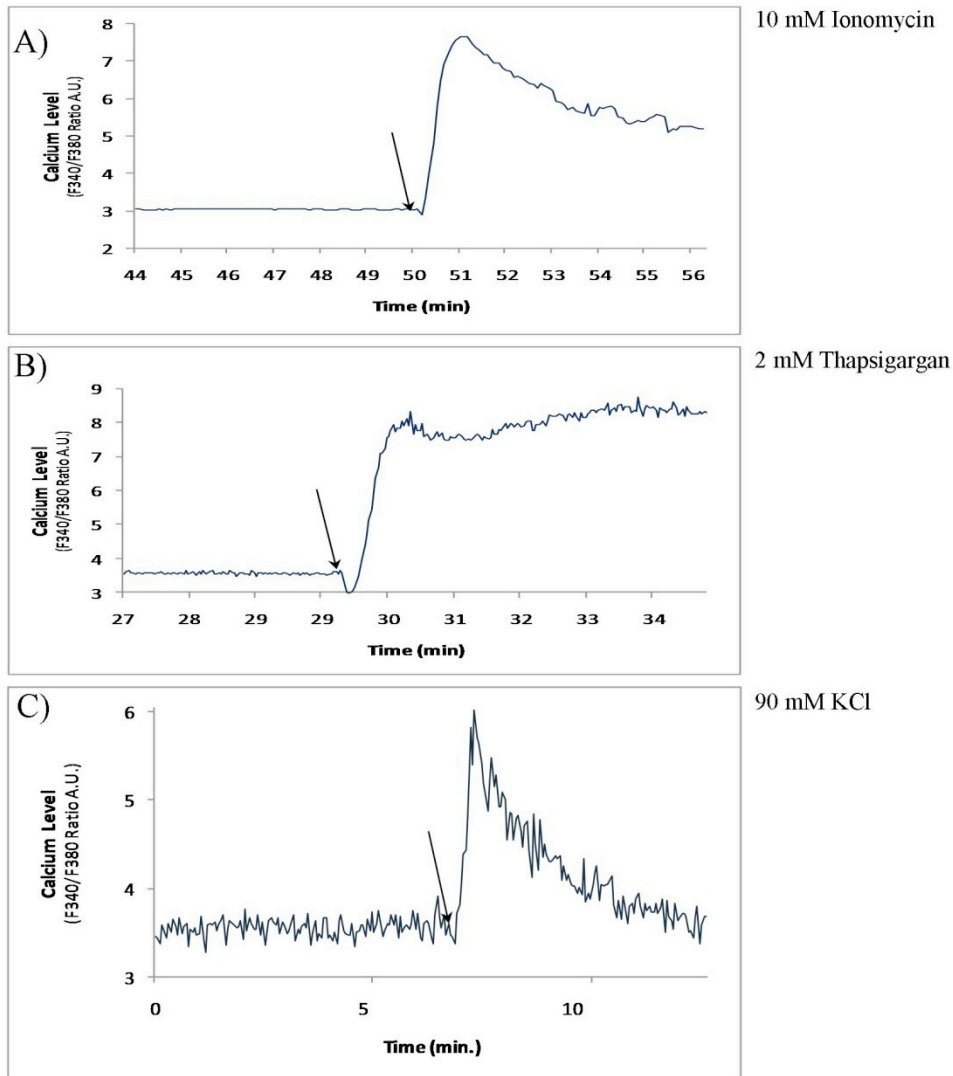


Figure 13. Calcium Response of bEnd3 Cells to Positive Controls. bEnd3 cells were allowed to equilibrate in Locke's buffer until a steady baseline was achieved. Once steady cells were treated with either 10 mM ionomycin (A), 2 mM Thapsigargin (B) or 90 mM KCl (C). The arrow indicates the time point at which cells were dosed. Calcium levels were determined by the ratio between fluorescence at 340 nm and 380 nm with FURA-2. An increase in this ratio is indicative of an increase in intracellular calcium.

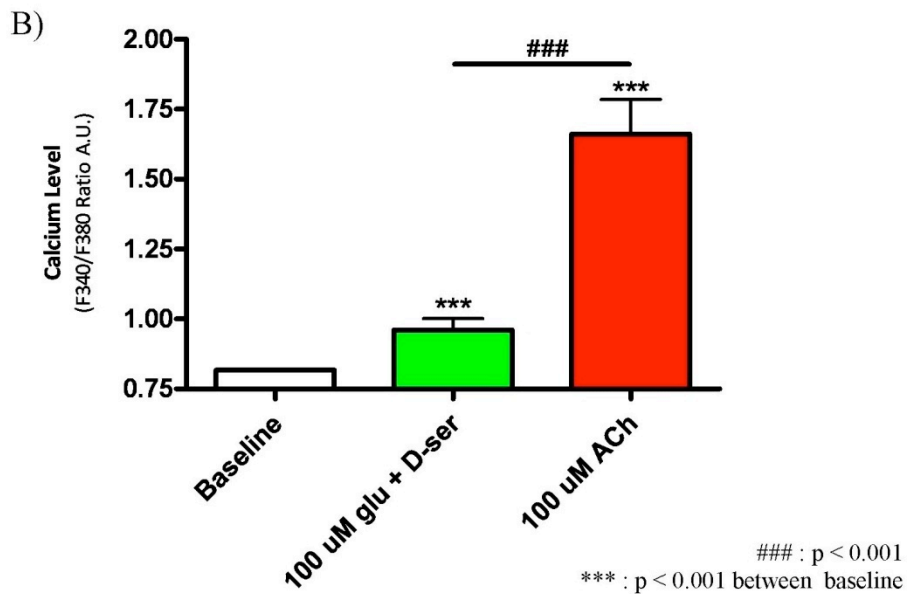
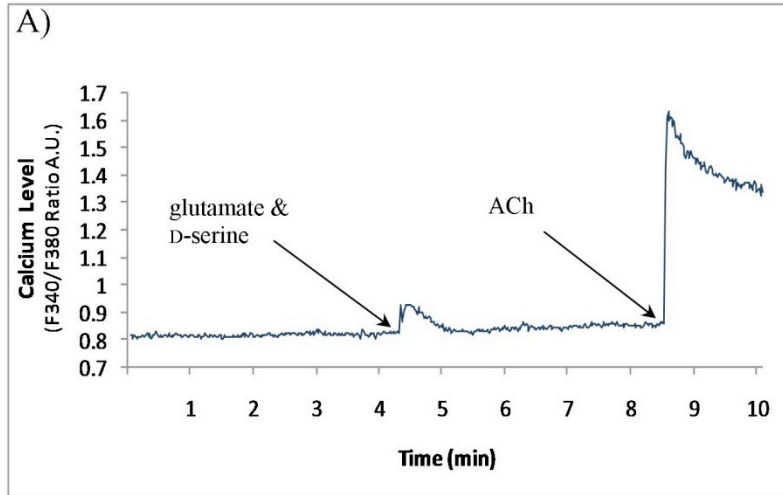


Figure 14. Calcium Response of bEnd3 Cells to Glutamate and D-Serine Treatment. A) bEnd3 cells were allowed to equilibrate in Locke's buffer before treatment with 100μM NMDAR coagonists D-serine and glutamate. After a baseline following NMDAR agonist treatment was established cells were treated with 100μM acetylcholine (ACh). An increase in this ratio is indicative of an increase in intracellular calcium. Arrows indicate point of treatment for NMDAR agonists (glutamate & D-serine) or ACh. B) Maximum increase in intracellular calcium for bEnd3 cells treated with either 100 μM glutamate and D-serine (green) or 100 μM ACh (red). P-values were determined by comparing both treatment groups to baseline conditions and comparing glutamate and D-serine treatment to ACh.

DISCUSSION

bEnd.3 Cells Express NMDAR Receptors

We found molecular and pharmacological evidence that strongly suggests that the bEnd.3 cell line expresses NMDARs. PCR data showed amplification of the NR1 subunit. This is critically important as all functional NMDARs necessitate the presence of the NR1 subunit, for both assembly and function. PCR primers were selected that amplified all of the 8 possible splice variants for NR1 so it was impossible to tell from PCR alone which variants of NR1 were expressed. Furthermore, using PCR, mRNA transcripts were detected for the NR2B, NR2C, NR2D and NR3B subunits. This is also supportive molecular evidence for NMDARs, as the tetrameric NMDA receptors require two additional subunits as combinations of NR2 and/or NR3.

Western blotting data using bEnd.3 homogenates resolved bands of the expected size for NR1 – the pan-NMDAR subunit – in the bEnd.3 cell line. We also found solid evidence for the presence of NR2C, which is important because it support other work done in our lab showing that NR2C is present in brain endothelium *in situ*. While PCR amplification of mRNA showed transcripts for NR2B and NR2D, no immunoreactive products were observed using antibodies for either subunit. This suggests that End3 cells contain transcripts for these subunits but they are not translated into protein. NR2A and NR3A gave multiple bands, none of which fell within 10 kDa of the expected sizes.

Coupled with the lack of supporting PCR transcripts it is unlikely that these two subunits are present. Finally, while PCR data supported the expression of NR3B, the immunoreactive product on western blots using an NR3B antibody was smaller than the expected size shown to be present in brain positive control tissue, by ~ 5 kDa. Two possibilities for this finding exist. First, similar to NR2B and NR2D, mRNA transcripts but not translated protein may be present in bEnd.3 cells. Second, it is possible that the translated product for NR3B does exist but post-translational modification of NR3B occurs differentially between the bEnd.3 cell line and mouse brain tissues. Some important post-translational modifications that may have produced the small alterations in size of NR3B *in vivo* include glycosylation and phosphorylation. Glycosylation of the NMDARs is a possible cause for larger than expected sized bands. NMDARs possess a number of potential consensus sites for either N-glycosylation (N-X-S/T, where X ≠ P; Everts et al., 1997) that occurs at asparagine residues or O-glycosylation at threonine or serine residues (Kleene and Schachner, 2004). Phosphorylation of residues in NMDAR subunits is also reported to occur in many instances (Cull-Candy et al., 2001; Scott et al., 2001; Yamakura and Shimoji, 1999).

Results are largely consistent with what others have discovered. The Scott group found evidence for the NR1 in bEnd.3 cells using western blot (Scott et al., 2007). Our results go beyond NR1 in these cells for the first time to demonstrate the existence of NR2C. Additional western immunoblots with

lysates from cultured human endothelial cells provided evidence supporting the existence of the NR1 subunit (Sharp et al., 2003). Betzen et al. (2009) also confirm our results regarding amplification of mRNA transcripts for NR1, NR2B, NR2C and NR2D. We are however the first group to show amplification of the NR3B subunit transcript.

We also found functional evidence supporting the presence of endothelial NMDARs using calcium imaging and protein nitrosylation studies. A small but significant increase in intracellular calcium levels was detected following treatment of the bEnd.3 cell line with both NMDA receptor agonists glutamate and D-serine. This is consistent with the function of NMDARs, which require glutamate and a co-agonist to function. Protein nitrosylation was also reduced significantly in the presence of the specific NMDAR antagonists AP5 and DCKA but not in the presence of the mGluR antagonist CNQX.

Based on structural and functional evidence, we believe that endothelial NMDARs expressed in bEnd.3 cells consist of two NR1 subunits and at least one NR2C subunit. We have strong evidence to support the presence of NR2C in endothelial NMDARs, which includes immunoblotting using an NR2C antibody, PCR amplification of NR2C mRNA, the low permeability to Ca^{2+} observed in the calcium imaging experiments and supporting data found in primary endothelial cells and brain slices collected by other members of our laboratory. In primary endothelial cells (cells cultured directly from mice) we have demonstrated

protein-protein interactions between NR1 and NR2C using NR2C antibodies. We have also seen immunoreactivity between NR2C antibodies and blood vessels in brain slices. Either an NR2 or NR3 subunit completes the tetramer, but it is unclear which. Coexposure of bEnd.3 cells to glutamate/D-serine with selective NR2 inhibitors as described in Table 1 would be useful in exposing the identity of a second NR2 subunit that make the channel. For studies examining the expression profile of NMDARs in native mouse brain tissue, western blotting of capillary enriched brain homogenates using the capillary depletion method first described by Triguero et al. (Triguero et al., 1990) could be employed. In the future, experiments in primary brain endothelial cells will allow us to collect data under more physiological relevant conditions.

Activation of bEnd.3 NMDARs Causes an eNOS-Independent Increase in Protein Nitrosylation

To test whether activation of NMDARs in the bEnd.3 cells line would activate eNOS, we used two methods: the Griess method, which is an assay that measures nitrite concentration in solution: nitrite is a chemical product produced when NO reacts with soluble oxygen. We also used slot blotting for protein nitrosylation. The Griess assay showed that glutamate and D-serine were not capable of increasing levels of nitrite over a 48-hour period. This indicates that either little or no eNOS activation results from NMDAR activation

in these cells or that NO is quickly scavenged. A large increase in protein nitrosylation was observed when we combined glutamate and D-serine. We originally hypothesized that activation of endothelial NMDARs would result in eNOS mediated production of NO. Two lines of evidence argue for rejection of this hypothesis. First, Failure to detect NMDAR-induced NO production using the Griess reaction indicated that eNOS is not activated significantly by glutamate and D-serine. Second, we were unable to reduce protein nitrosylation using the eNOS inhibitor L-NIO. An alternative explanation for our results is that exposure to glutamate and D-serine led to superoxide production that, in turn, resulted in increased production of peroxynitrite and nitrosylative stress. This is supported by previous observations that NMDA receptors increase oxidative stress (Bossy-Wetzel et al., 2004; Nelson et al., 2003; Uehara et al., 2006). The response seen in our bEnd.3 cells is under conditions representative of pathophysiological states. In our model, bEnd.3 cells are continuous exposure to elevated levels of glutamate/D-serine over a 24 hours period before any effect is observed. Continuous exposure to glutamate levels of similar magnitude in brain occur only during excitotoxic events.

Another explanation for the observed increase in nitrosylation in the presence of an eNOS-selective inhibitor is the activation of another NOS isoform. iNOS expression may be induced in endothelial cells following exposure to substances such as tumour necrosis factor- α (Beasley et al., 1991;

Nathan, 1992). Furthermore, the expression profiles of eNOS and iNOS have been shown to change with passage number in the human umbilical vein endothelial cell (HUVEC) line (Yoon et al., 2010). It is possible that bEnd.3 cells behave in a similar fashion. With increasing passage numbers bEnd.3 cells increase expression of iNOS while levels of eNOS within the cell diminish. Exposure of bEnd.3 cells to glutamate and D-serine could then explain the observed inability of L-NIO to prevent the rise in protein nitrosylation. The NMDAR-dependent activation of iNOS has been shown to occur in glial cells (Buskila and Amitai, 2010). Activation of mitochondrial NOS (Elfering et al., 2002; Leite et al., 2010) is yet another alternative explanation that does not require eNOS. In this model, activation of endothelial NMDARs initiates peroxynitrite formation from superoxide and NO, both produced in the mitochondria. Even though non eNOS sources of NO are possibilities, we reiterate that Griess assays produced no evidence of glutamate/D-serine-mediated NO accumulation.

CONCLUSION

Overall, our experiments showed that the bEnd.3 cell line does express functional NMDARs. Notably they express the essential NR1 subunit as well as NR2C. Exposure of the bEnd.3 cell line to NMDAR agonists caused a modest increase in intracellular calcium levels. This increase in calcium did not stimulate the production of NO through eNOS, as indicated by the Griess reaction. However, we did observe a glutamate and D-serine induced increase in protein nitrosylation. The increase in nitrosylated tyrosine residues was demonstrated to be NMDAR-dependent as the effect was reduced significantly by NMDAR blockade using the glutamate site antagonist AP5 and glycine site antagonist DCKA.

REFERENCES

Agbaje, I. M., McVicar, C. M., Schock, B. C., McClure, N., Atkinson, A. B., Rogers, D., and Lewis, S. E.: Increased concentrations of the oxidative DNA adduct 7,8-dihydro-8-oxo-2-deoxyguanosine in the germ-line of men with type 1 diabetes. *Reprod Biomed Online* **16** (3): 401-9, 2008.

Anderson, C. M., Bergher, J. P., and Swanson, R. A.: ATP-induced ATP release from astrocytes. *J Neurochem* **88** (1): 246-56, 2004.

Anson, L. C., Chen, P. E., Wyllie, D. J., Colquhoun, D., and Schoepfer, R.: Identification of amino acid residues of the NR2A subunit that control glutamate potency in recombinant NR1/NR2A NMDA receptors. *J Neurosci* **18** (2): 581-9, 1998.

Anson, L. C., Schoepfer, R., Colquhoun, D., and Wyllie, D. J.: Single-channel analysis of an NMDA receptor possessing a mutation in the region of the glutamate binding site. *J Physiol* **527 Pt 2**: 225-37, 2000.

Archer, S.: Measurement of nitric oxide in biological models. *Faseb J* **7** (2): 349-60, 1993.

Awobuluyi, M., Yang, J., Ye, Y., Chatterton, J. E., Godzik, A., Lipton, S. A., and Zhang, D.: Subunit-specific roles of glycine-binding domains in activation of NR1/NR3 N-methyl-D-aspartate receptors. *Mol Pharmacol* **71** (1): 112-22, 2007.

Beasley, D., Schwartz, J. H., and Brenner, B. M.: Interleukin 1 induces prolonged L-arginine-dependent cyclic guanosine monophosphate and nitrite production in rat vascular smooth muscle cells. *J Clin Invest* **87** (2): 602-8, 1991.

Bennett, J. A., and Dingledine, R.: Topology profile for a glutamate receptor: three transmembrane domains and a channel-lining reentrant membrane loop. *Neuron* **14** (2): 373-84, 1995.

Betzen, C., White, R., Zehendner, C. M., Pietrowski, E., Bender, B., Luhmann, H. J., and Kuhlmann, C. R.: Oxidative stress upregulates the NMDA receptor on cerebrovascular endothelium. *Free Radic Biol Med* **47** (8): 1212-20, 2009.

Bezzi, P., Carmignoto, G., Pasti, L., Vesce, S., Rossi, D., Rizzini, B. L., Pozzan, T., and Volterra, A.: Prostaglandins stimulate calcium-dependent glutamate release in astrocytes. *Nature* **391** (6664): 281-5, 1998.

Bossy-Wetzell, E., Schwarzenbacher, R., and Lipton, S. A.: Molecular pathways to neurodegeneration. *Nat Med* **10 Suppl**: S2-9, 2004.

Bradford, M. M.: A rapid and sensitive method for the quantitation of microgram quantities of protein utilizing the principle of protein-dye binding. *Anal Biochem* **72**: 248-54, 1976.

Brimecombe, J. C., Gallagher, M. J., Lynch, D. R., and Aizenman, E.: An NR2B point mutation affecting haloperidol and CP101,606 sensitivity of single recombinant N-methyl-D-aspartate receptors. *J Pharmacol Exp Ther* **286** (2): 627-34, 1998.

Burney, S., Caulfield, J. L., Niles, J. C., Wishnok, J. S., and Tannenbaum, S. R.: The chemistry of DNA damage from nitric oxide and peroxynitrite. *Mutat Res* **424** (1-2): 37-49, 1999.

Bushong, E. A., Martone, M. E., Jones, Y. Z., and Ellisman, M. H.: Protoplasmic astrocytes in CA1 stratum radiatum occupy separate anatomical domains. *J Neurosci* **22** (1): 183-92, 2002.

Buskila, Y., and Amitai, Y.: Astrocytic iNOS-dependent enhancement of synaptic release in mouse neocortex. *J Neurophysiol* **103** (3): 1322-8, 2010.

Cavara, N. A., Orth, A., and Hollmann, M.: Effects of NR1 splicing on NR1/NR3B-type excitatory glycine receptors. *BMC Neurosci* **10**: 32, 2009.

Chatterton, J. E., Awobuluyi, M., Premkumar, L. S., Takahashi, H., Talantova, M., Shin, Y., Cui, J., Tu, S., Sevarino, K. A., Nakanishi, N., Tong, G., Lipton, S. A., and Zhang, D.: Excitatory glycine receptors containing the NR3 family of NMDA receptor subunits. *Nature* **415** (6873): 793-8, 2002.

Choi, Y. B., Tenneti, L., Le, D. A., Ortiz, J., Bai, G., Chen, H. S., and Lipton, S. A.: Molecular basis of NMDA receptor-coupled ion channel modulation by S-nitrosylation. *Nat Neurosci* **3** (1): 15-21, 2000.

Coco, S., Calegari, F., Pravettoni, E., Pozzi, D., Taverna, E., Rosa, P., Matteoli, M., and Verderio, C.: Storage and release of ATP from astrocytes in culture. *J Biol Chem* **278** (2): 1354-62, 2003.

Cornell-Bell, A. H., Finkbeiner, S. M., Cooper, M. S., and Smith, S. J.: Glutamate induces calcium waves in cultured astrocytes: long-range glial signaling. *Science* **247** (4941): 470-3, 1990.

Covasa, M., Ritter, R. C., and Burns, G. A.: NMDA receptor participation in control of food intake by the stomach. *Am J Physiol Regul Integr Comp Physiol* **278** (5): R1362-8, 2000.

Cull-Candy, S., Brickley, S., and Farrant, M.: NMDA receptor subunits: diversity, development and disease. *Curr Opin Neurobiol* **11** (3): 327-35, 2001.

Darby, M., Kuzmiski, J. B., Panenka, W., Feighan, D., and MacVicar, B. A.: ATP released from astrocytes during swelling activates chloride channels. *J Neurophysiol* **89** (4): 1870-7, 2003.

Das, S., Sasaki, Y. F., Rothe, T., Premkumar, L. S., Takasu, M., Crandall, J. E., Dikkes, P., Conner, D. A., Rayudu, P. V., Cheung, W., Chen, H. S., Lipton, S. A., and Nakanishi, N.: Increased NMDA current and spine density in mice lacking the NMDA receptor subunit NR3A. *Nature* **393** (6683): 377-81, 1998.

Deng, A., and Thomson, S. C.: Renal NMDA receptors independently stimulate proximal reabsorption and glomerular filtration. *Am J Physiol Renal Physiol* **296** (5): F976-82, 2009.

Deng, A., Valdivielso, J. M., Munger, K. A., Blantz, R. C., and Thomson, S. C.: Vasodilatory N-methyl-D-aspartate receptors are constitutively expressed in rat kidney. *J Am Soc Nephrol* **13** (5): 1381-4, 2002.

Dingledine, R., Borges, K., Bowie, D., and Traynelis, S. F.: The glutamate receptor ion channels. *Pharmacol Rev* **51** (1): 7-61, 1999.

Domoki, F., Kis, B., Gaspar, T., Bari, F., and Busija, D. W.: Cerebromicrovascular endothelial cells are resistant to L-glutamate. *Am J Physiol Regul Integr Comp Physiol* **295** (4): R1099-108, 2008.

Donevan, S. D., and McCabe, R. T.: Conantokin G is an NR2B-selective competitive antagonist of N-methyl-D-aspartate receptors. *Mol Pharmacol* **58** (3): 614-23, 2000.

Drake, C. T., and Iadecola, C.: The role of neuronal signaling in controlling cerebral blood flow. *Brain Lang* **102** (2): 141-52, 2007.

Durand, G. M., Bennett, M. V., and Zukin, R. S.: Splice variants of the N-methyl-D-aspartate receptor NR1 identify domains involved in regulation by polyamines and protein kinase C. *Proc Natl Acad Sci U S A* **90** (14): 6731-5, 1993.

Elfering, S. L., Sarkela, T. M., and Giulivi, C.: Biochemistry of mitochondrial nitric-oxide synthase. *J Biol Chem* **277** (41): 38079-86, 2002.

Everts, I., Villmann, C., and Hollmann, M.: N-Glycosylation is not a prerequisite for glutamate receptor function but is essential for lectin modulation. *Mol Pharmacol* **52** (5): 861-73, 1997.

Faraci, F. M., and Heistad, D. D.: Regulation of large cerebral arteries and cerebral microvascular pressure. *Circ Res* **66** (1): 8-17, 1990.

Fisher, M.: Pericyte signaling in the neurovascular unit. *Stroke* **40** (3 Suppl): S13-5, 2009.

Fotuhi, M., Hachinski, V., and Whitehouse, P. J.: Changing perspectives regarding late-life dementia. *Nat Rev Neurol* **5** (12): 649-58, 2009.

Gao, X., Xu, X., Pang, J., Zhang, C., Ding, J. M., Peng, X., Liu, Y., and Cao, J. M.: NMDA receptor activation induces mitochondrial dysfunction, oxidative stress and apoptosis in cultured neonatal rat cardiomyocytes. *Physiol Res* **56** (5): 559-69, 2007.

Garvey, E. P., Oplinger, J. A., Furfine, E. S., Kiff, R. J., Laszlo, F., Whittle, B. J., and Knowles, R. G.: 1400W is a slow, tight binding, and highly selective inhibitor of inducible nitric-oxide synthase in vitro and in vivo. *J Biol Chem* **272** (8): 4959-63, 1997.

Gill, R., Tsung, A., and Billiar, T.: Linking oxidative stress to inflammation: Toll-like receptors. *Free Radic Biol Med* **48** (9): 1121-32, 2010.

Gill, S., Veinot, J., Kavanagh, M., and Pulido, O.: Human heart glutamate receptors - implications for toxicology, food safety, and drug discovery. *Toxicol Pathol* **35** (3): 411-7, 2007.

Gomez-Rodriguez, J., Washington, V., Cheng, J., Dutra, A., Pak, E., Liu, P., McVicar, D. W., and Schwartzberg, P. L.: Advantages of q-PCR as a method of screening for gene targeting in mammalian cells using conventional and whole BAC-based constructs. *Nucleic Acids Res* **36** (18): e117, 2008.

Gordon, G. R., Choi, H. B., Rungta, R. L., Ellis-Davies, G. C., and MacVicar, B. A.: Brain metabolism dictates the polarity of astrocyte control over arterioles. *Nature* **456** (7223): 745-9, 2008.

Green, L. C., Wagner, D. A., Glogowski, J., Skipper, P. L., Wishnok, J. S., and Tannenbaum, S. R.: Analysis of nitrate, nitrite, and [15N]nitrate in biological fluids. *Anal Biochem* **126** (1): 131-8, 1982.

Gulbenkian, S., Uddman, R., and Edvinsson, L.: Neuronal messengers in the human cerebral circulation. *Peptides* **22** (6): 995-1007, 2001.

Halassa, M. M., Fellin, T., Takano, H., Dong, J. H., and Haydon, P. G.: Synaptic islands defined by the territory of a single astrocyte. *J Neurosci* **27** (24): 6473-7, 2007.

Harder, D. R., Alkayed, N. J., Lange, A. R., Gebremedhin, D., and Roman, R. J.: Functional hyperemia in the brain: hypothesis for astrocyte-derived vasodilator metabolites. *Stroke* **29** (1): 229-34, 1998.

Hashimoto, A., Oka, T., and Nishikawa, T.: Extracellular concentration of endogenous free D-serine in the rat brain as revealed by in vivo microdialysis. *Neuroscience* **66** (3): 635-43, 1995.

Hess, D. T., Matsumoto, A., Kim, S. O., Marshall, H. E., and Stamler, J. S.: Protein S-nitrosylation: purview and parameters. *Nat Rev Mol Cell Biol* **6** (2): 150-66, 2005.

Hinoi, E., Fujimori, S., and Yoneda, Y.: Modulation of cellular differentiation by N-methyl-D-aspartate receptors in osteoblasts. *Faseb J* **17** (11): 1532-4, 2003.

Hirase, H.: A multi-photon window onto neuronal-glial-vascular communication. *Trends Neurosci* **28** (5): 217-9, 2005.

Hossmann, K. A.: Pathophysiology and therapy of experimental stroke. *Cell Mol Neurobiol* **26** (7-8): 1057-83, 2006.

Hrabetova, S., Serrano, P., Blace, N., Tse, H. W., Skifter, D. A., Jane, D. E., Monaghan, D. T., and Sacktor, T. C.: Distinct NMDA receptor subpopulations contribute to long-term potentiation and long-term depression induction. *J Neurosci* **20** (12): RC81, 2000.

Hu, J., Wang, Z., Guo, Y. Y., Zhang, X. N., Xu, Z. H., Liu, S. B., Guo, H. J., Yang, Q., Zhang, F. X., Sun, X. L., and Zhao, M. G.: A role of periaqueductal grey NR2B-containing NMDA receptor in mediating persistent inflammatory pain. *Mol Pain* **5**: 71, 2009.

Iadecola, C.: Neurovascular regulation in the normal brain and in Alzheimer's disease. *Nat Rev Neurosci* **5** (5): 347-60, 2004.

Iadecola, C.: The overlap between neurodegenerative and vascular factors in the pathogenesis of dementia. *Acta Neuropathol* **120** (3): 287-96, 2010.

Iadecola, C., and Nedergaard, M.: Glial regulation of the cerebral microvasculature. *Nat Neurosci* **10** (11): 1369-76, 2007.

Ilyin, V. I., Whittemore, E. R., Guastella, J., Weber, E., and Woodward, R. M.: Subtype-selective inhibition of N-methyl-D-aspartate receptors by haloperidol. *Mol Pharmacol* **50** (6): 1541-50, 1996.

Inagaki, N., Kuromi, H., Gono, T., Okamoto, Y., Ishida, H., Seino, Y., Kaneko, T., Iwanaga, T., and Seino, S.: Expression and role of ionotropic glutamate receptors in pancreatic islet cells. *FASEB J* **9** (8): 686-91, 1995.

Jones, E. G.: On the mode of entry of blood vessels into the cerebral cortex. *J Anat* **106** (Pt 3): 507-20, 1970.

Kalaria, R. N.: Cerebrovascular degeneration is related to amyloid-beta protein deposition in Alzheimer's disease. *Ann N Y Acad Sci* **826**: 263-71, 1997.

Karadottir, R., Cavalier, P., Bergersen, L. H., and Attwell, D.: NMDA receptors are expressed in oligodendrocytes and activated in ischaemia. *Nature* **438** (7071): 1162-6, 2005.

Kemp, N., and Bashir, Z. I.: Long-term depression: a cascade of induction and expression mechanisms. *Prog Neurobiol* **65** (4): 339-65, 2001.

Kew, J. N., Trube, G., and Kemp, J. A.: State-dependent NMDA receptor antagonism by Ro 8-4304, a novel NR2B selective, non-competitive, voltage-independent antagonist. *Br J Pharmacol* **123** (3): 463-72, 1998.

Kim, P. M., Aizawa, H., Kim, P. S., Huang, A. S., Wickramasinghe, S. R., Kashani, A. H., Barrow, R. K., Huganir, R. L., Ghosh, A., and Snyder, S. H.: Serine racemase: activation by glutamate neurotransmission via glutamate receptor interacting protein and mediation of neuronal migration. *Proc Natl Acad Sci U S A* **102** (6): 2105-10, 2005.

Kleckner, N. W., Glazewski, J. C., Chen, C. C., and Moscrip, T. D.: Subtype-selective antagonism of N-methyl-D-aspartate receptors by felbamate: insights into the mechanism of action. *J Pharmacol Exp Ther* **289** (2): 886-94, 1999.

Kleene, R., and Schachner, M.: Glycans and neural cell interactions. *Nat Rev Neurosci* **5** (3): 195-208, 2004.

Knowles, R. G., and Moncada, S.: Nitric oxide synthases in mammals. *Biochem J* **298** (Pt 2): 249-58, 1994.

Kohr, G.: NMDA receptor function: subunit composition versus spatial distribution. *Cell Tissue Res* **326** (2): 439-46, 2006.

Krebs, C., Fernandes, H. B., Sheldon, C., Raymond, L. A., and Baimbridge, K. G.: Functional NMDA receptor subtype 2B is expressed in astrocytes after ischemia in vivo and anoxia in vitro. *J Neurosci* **23** (8): 3364-72, 2003.

Krimer, L. S., Muly, E. C., 3rd, Williams, G. V., and Goldman-Rakic, P. S.: Dopaminergic regulation of cerebral cortical microcirculation. *Nat Neurosci* **1** (4): 286-9, 1998.

Krizbai, I. A., Deli, M. A., Pestenacz, A., Siklos, L., Szabo, C. A., Andras, I., and Joo, F.: Expression of glutamate receptors on cultured cerebral endothelial cells. *J Neurosci Res* **54** (6): 814-9, 1998.

Kuryatov, A., Laube, B., Betz, H., and Kuhse, J.: Mutational analysis of the glycine-binding site of the NMDA receptor: structural similarity with bacterial amino acid-binding proteins. *Neuron* **12** (6): 1291-300, 1994.

Lalo, U., Pankratov, Y., Kirchhoff, F., North, R. A., and Verkhratsky, A.: NMDA receptors mediate neuron-to-glia signaling in mouse cortical astrocytes. *J Neurosci* **26** (10): 2673-83, 2006.

Laube, B., Kuhse, J., and Betz, H.: Evidence for a tetrameric structure of recombinant NMDA receptors. *J Neurosci* **18** (8): 2954-61, 1998.

Leiper, J., Murray-Rust, J., McDonald, N., and Vallance, P.: S-nitrosylation of dimethylarginine dimethylaminohydrolase regulates enzyme activity: further interactions between nitric oxide synthase and dimethylarginine dimethylaminohydrolase. *Proc Natl Acad Sci U S A* **99** (21): 13527-32, 2002.

Leite, A. C., Oliveira, H. C., Utino, F. L., Garcia, R., Alberici, L. C., Fernandes, M. P., Castilho, R. F., and Vercesi, A. E.: Mitochondria generated nitric oxide protects against permeability transition via formation of membrane protein S-nitrosothiols. *Biochim Biophys Acta* **1797** (6-7): 1210-6, 2010.

Leung, J. C., Marphis, T., Craver, R. D., and Silverstein, D. M.: Altered NMDA receptor expression in renal toxicity: Protection with a receptor antagonist. *Kidney Int* **66** (1): 167-76, 2004.

Li, C. Q., Pang, B., Kiziltepe, T., Trudel, L. J., Engelward, B. P., Dedon, P. C., and Wogan, G. N.: Threshold effects of nitric oxide-induced toxicity and cellular responses in wild-type and p53-null human lymphoblastoid cells. *Chem Res Toxicol* **19** (3): 399-406, 2006.

Li, D., Ropert, N., Koulakoff, A., Giaume, C., and Oheim, M.: Lysosomes are the major vesicular compartment undergoing Ca²⁺-regulated exocytosis from cortical astrocytes. *J Neurosci* **28** (30): 7648-58, 2008.

Lipton, S. A., Choi, Y. B., Pan, Z. H., Lei, S. Z., Chen, H. S., Sucher, N. J., Loscalzo, J., Singel, D. J., and Stamler, J. S.: A redox-based mechanism for the neuroprotective and neurodestructive effects of nitric oxide and related nitroso-compounds. *Nature* **364** (6438): 626-32, 1993.

Lipton, S. A., Choi, Y. B., Takahashi, H., Zhang, D., Li, W., Godzik, A., and Bankston, L. A.: Cysteine regulation of protein function--as exemplified by NMDA-receptor modulation. *Trends Neurosci* **25** (9): 474-80, 2002.

Liu, J., Evans, M. S., Brewer, G. J., and Lee, T. J.: N-type Ca²⁺ channels in cultured rat sphenopalatine ganglion neurons: an immunohistochemical and electrophysiological study. *J Cereb Blood Flow Metab* **20** (1): 183-91, 2000.

Liu, L., Wong, T. P., Pozza, M. F., Lingenhoehl, K., Wang, Y., Sheng, M., Auberson, Y. P., and Wang, Y. T.: Role of NMDA receptor subtypes in governing the direction of hippocampal synaptic plasticity. *Science* **304** (5673): 1021-4, 2004.

Madry, C., Mesic, I., Bartholomaeus, I., Nicke, A., Betz, H., and Laube, B.: Principal role of NR3 subunits in NR1/NR3 excitatory glycine receptor function. *Biochem Biophys Res Commun* **354** (1): 102-8, 2007.

Massey, P. V., Johnson, B. E., Moulton, P. R., Auberson, Y. P., Brown, M. W., Molnar, E., Collingridge, G. L., and Bashir, Z. I.: Differential roles of NR2A and NR2B-containing NMDA receptors in cortical long-term potentiation and long-term depression. *J Neurosci* **24** (36): 7821-8, 2004.

Mayer, B., Pfeiffer, S., Schrammel, A., Koesling, D., Schmidt, K., and Brunner, F.: A new pathway of nitric oxide/cyclic GMP signaling involving S-nitrosoglutathione. *J Biol Chem* **273** (6): 3264-70, 1998.

McCarthy, K. D., and de Vellis, J.: Alpha-adrenergic receptor modulation of beta-adrenergic, adenosine and prostaglandin E1 increased adenosine 3':5'-cyclic monophosphate levels in primary cultures of glia. *J Cyclic Nucleotide Res* **4** (1): 15-26, 1978.

McIlhinney, R. A., Philipps, E., Le Bourdelles, B., Grimwood, S., Wafford, K., Sandhu, S., and Whiting, P.: Assembly of N-methyl-D-aspartate (NMDA) receptors. *Biochem Soc Trans* **31** (Pt 4): 865-8, 2003.

McNearney, T. A., Ma, Y., Chen, Y., Tagliatela, G., Yin, H., Zhang, W. R., and Westlund, K. N.: A peripheral neuroimmune link: glutamate agonists upregulate NMDA NR1 receptor mRNA and protein, vimentin, TNF-alpha, and RANTES in cultured human synoviocytes. *Am J Physiol Regul Integr Comp Physiol* **298** (3): R584-98, 2010.

Mentis, M. J., Horwitz, B., Grady, C. L., Alexander, G. E., VanMeter, J. W., Maisog, J. M., Pietrini, P., Schapiro, M. B., and Rapoport, S. I.: Visual cortical dysfunction in Alzheimer's disease evaluated with a temporally graded "stress test" during PET. *Am J Psychiatry* **153** (1): 32-40, 1996.

Momiyama, A., Feldmeyer, D., and Cull-Candy, S. G.: Identification of a native low-conductance NMDA channel with reduced sensitivity to Mg²⁺ in rat central neurones. *J Physiol* **494** (Pt 2): 479-92, 1996.

Monyer, H., Burnashev, N., Laurie, D. J., Sakmann, B., and Seeburg, P. H.: Developmental and regional expression in the rat brain and functional properties of four NMDA receptors. *Neuron* **12** (3): 529-40, 1994.

Morhenn, V. B., Waleh, N. S., Mansbridge, J. N., Unson, D., Zolotarev, A., Cline, P., and Toll, L.: Evidence for an NMDA receptor subunit in human keratinocytes and rat cardiocytes. *Eur J Pharmacol* **268** (3): 409-14, 1994.

Morley, P., Small, D. L., Murray, C. L., Mealing, G. A., Poulter, M. O., Durkin, J. P., and Stanimirovic, D. B.: Evidence that functional glutamate receptors are not expressed on rat or human cerebromicrovascular endothelial cells. *J Cereb Blood Flow Metab* **18** (4): 396-406, 1998.

Mothet, J. P., Parent, A. T., Wolosker, H., Brady, R. O., Jr., Linden, D. J., Ferris, C. D., Rogawski, M. A., and Snyder, S. H.: D-serine is an endogenous ligand for the glycine site of the N-methyl-D-aspartate receptor. *Proc Natl Acad Sci U S A* **97** (9): 4926-31, 2000.

Mothet, J. P., Pollegioni, L., Ouanounou, G., Martineau, M., Fossier, P., and Baux, G.: Glutamate receptor activation triggers a calcium-dependent and SNARE protein-dependent release of the gliotransmitter D-serine. *Proc Natl Acad Sci U S A* **102** (15): 5606-11, 2005.

Mulligan, S. J., and MacVicar, B. A.: Calcium transients in astrocyte endfeet cause cerebrovascular constrictions. *Nature* **431** (7005): 195-9, 2004.

Nagy, J.: The NR2B subtype of NMDA receptor: a potential target for the treatment of alcohol dependence. *Curr Drug Targets CNS Neurol Disord* **3** (3): 169-79, 2004.

Nathan, C.: Nitric oxide as a secretory product of mammalian cells. *FASEB J* **6** (12): 3051-64, 1992.

Nelson, E. J., Connolly, J., and McArthur, P.: Nitric oxide and S-nitrosylation: excitotoxic and cell signaling mechanism. *Biol Cell* **95** (1): 3-8, 2003.

Newman, E. A., Frambach, D. A., and Odette, L. L.: Control of extracellular potassium levels by retinal glial cell K⁺ siphoning. *Science* **225** (4667): 1174-5, 1984.

Nguyen, T., Brunson, D., Crespi, C. L., Penman, B. W., Wishnok, J. S., and Tannenbaum, S. R.: DNA damage and mutation in human cells exposed to nitric oxide in vitro. *Proc Natl Acad Sci U S A* **89** (7): 3030-4, 1992.

Niwa, K., Araki, E., Morham, S. G., Ross, M. E., and Iadecola, C.: Cyclooxygenase-2 contributes to functional hyperemia in whisker-barrel cortex. *J Neurosci* **20** (2): 763-70, 2000.

Papadakis, M., Hawkins, L. M., and Stephenson, F. A.: Appropriate NR1-NR1 disulfide-linked homodimer formation is requisite for efficient expression of functional, cell surface N-methyl-D-aspartate NR1/NR2 receptors. *J Biol Chem* **279** (15): 14703-12, 2004.

Park, L., Anrather, J., Forster, C., Kazama, K., Carlson, G. A., and Iadecola, C.: Abeta-induced vascular oxidative stress and attenuation of functional hyperemia in mouse somatosensory cortex. *J Cereb Blood Flow Metab* **24** (3): 334-42, 2004.

Parpura, V., Basarsky, T. A., Liu, F., Jeftinija, K., Jeftinija, S., and Haydon, P. G.: Glutamate-mediated astrocyte-neuron signalling. *Nature* **369** (6483): 744-7, 1994.

Patel, J. M., Zhang, J., and Block, E. R.: Nitric oxide-induced inhibition of lung endothelial cell nitric oxide synthase via interaction with allosteric thiols: role of thioredoxin in regulation of catalytic activity. *Am J Respir Cell Mol Biol* **15** (3): 410-9, 1996.

Porter, J. T., and McCarthy, K. D.: Astrocytic neurotransmitter receptors in situ and in vivo. *Prog Neurobiol* **51** (4): 439-55, 1997.

Preskorn, S. H., Baker, B., Kolluri, S., Menniti, F. S., Krams, M., and Landen, J. W.: An innovative design to establish proof of concept of the antidepressant effects of the NR2B subunit selective N-methyl-D-aspartate antagonist, CP-101,606, in patients with treatment-refractory major depressive disorder. *J Clin Psychopharmacol* **28** (6): 631-7, 2008.

Preston, E., Webster, J., and Palmer, G. C.: Lack of evidence for direct involvement of NMDA receptors or polyamines in blood-brain barrier injury after cerebral ischemia in rats. *Brain Res* **813** (1): 191-4, 1998.

Qian, A., Buller, A. L., and Johnson, J. W.: NR2 subunit-dependence of NMDA receptor channel block by external Mg²⁺. *J Physiol* **562** (Pt 2): 319-31, 2005.

Raichle, M. E., Hartman, B. K., Eichling, J. O., and Sharpe, L. G.: Central noradrenergic regulation of cerebral blood flow and vascular permeability. *Proc Natl Acad Sci U S A* **72** (9): 3726-30, 1975.

Ransom, R. W., and Stec, N. L.: Cooperative modulation of [3H]MK-801 binding to the N-methyl-D-aspartate receptor-ion channel complex by L-glutamate, glycine, and polyamines. *J Neurochem* **51** (3): 830-6, 1988.

Ravi, K., Brennan, L. A., Levic, S., Ross, P. A., and Black, S. M.: S-nitrosylation of endothelial nitric oxide synthase is associated with monomerization and decreased enzyme activity. *Proc Natl Acad Sci U S A* **101** (8): 2619-24, 2004.

Rodrigo, J., Springall, D. R., Uttenthal, O., Bentura, M. L., Abadia-Molina, F., Riveros-Moreno, V., Martinez-Murillo, R., Polak, J. M., and Moncada, S.: Localization of nitric oxide synthase in the adult rat brain. *Philos Trans R Soc Lond B Biol Sci* **345** (1312): 175-221, 1994.

Roy, C. S., and Sherrington, C. S.: On the Regulation of the Blood-supply of the Brain. *J Physiol* **11** (1-2): 85-158 17, 1890.

Salgo, M. G., Bermudez, E., Squadrito, G. L., and Pryor, W. A.: Peroxynitrite causes DNA damage and oxidation of thiols in rat thymocytes [corrected]. *Arch Biochem Biophys* **322** (2): 500-5, 1995.

Schell, M. J., Molliver, M. E., and Snyder, S. H.: D-serine, an endogenous synaptic modulator: localization to astrocytes and glutamate-stimulated release. *Proc Natl Acad Sci U S A* **92** (9): 3948-52, 1995.

Schuler, T., Mesic, I., Madry, C., Bartholomaeus, I., and Laube, B.: Formation of NR1/NR2 and NR1/NR3 heterodimers constitutes the initial step in N-methyl-D-aspartate receptor assembly. *J Biol Chem* **283** (1): 37-46, 2008.

Scott, D. B., Blanpied, T. A., Swanson, G. T., Zhang, C., and Ehlers, M. D.: An NMDA receptor ER retention signal regulated by phosphorylation and alternative splicing. *J Neurosci* **21** (9): 3063-72, 2001.

Scott, G. S., Bowman, S. R., Smith, T., Flower, R. J., and Bolton, C.: Glutamate-stimulated peroxynitrite production in a brain-derived endothelial cell line is dependent on N-methyl-D-aspartate (NMDA) receptor activation. *Biochem Pharmacol* **73** (2): 228-36, 2007.

Seeber, S., Becker, K., Rau, T., Eschenhagen, T., Becker, C. M., and Herkert, M.: Transient expression of NMDA receptor subunit NR2B in the developing rat heart. *J Neurochem* **75** (6): 2472-7, 2000.

Sharp, C. D., Hines, I., Houghton, J., Warren, A., Jackson, T. H. t., Jawahar, A., Nanda, A., Elrod, J. W., Long, A., Chi, A., Minagar, A., and Alexander, J. S.: Glutamate causes a loss in human cerebral endothelial barrier integrity through activation of NMDA receptor. *Am J Physiol Heart Circ Physiol* **285** (6): H2592-8, 2003.

Sharp, C. D., Houghton, J., Elrod, J. W., Warren, A., Jackson, T. H. t., Jawahar, A., Nanda, A., Minagar, A., and Alexander, J. S.: N-methyl-D-aspartate receptor activation in human cerebral endothelium promotes intracellular oxidant stress. *Am J Physiol Heart Circ Physiol* **288** (4): H1893-9, 2005.

Shiokawa, H., Kaftan, E. J., MacDermott, A. B., and Tong, C. K.: NR2 subunits and NMDA receptors on lamina II inhibitory and excitatory interneurons of the mouse dorsal horn. *Mol Pain* **6**: 26, 2010.

Smothers, C. T., and Woodward, J. J.: Pharmacological characterization of glycine-activated currents in HEK 293 cells expressing N-methyl-D-aspartate NR1 and NR3 subunits. *J Pharmacol Exp Ther* **322** (2): 739-48, 2007.

Somjen, G. G.: Nervenkitz: notes on the history of the concept of neuroglia. *Glia* **1** (1): 2-9, 1988.

Stamler, J. S., Simon, D. I., Osborne, J. A., Mullins, M. E., Jaraki, O., Michel, T., Singel, D. J., and Loscalzo, J.: S-nitrosylation of proteins with nitric oxide: synthesis and characterization of biologically active compounds. *Proc Natl Acad Sci U S A* **89** (1): 444-8, 1992.

Stamler, J. S., Toone, E. J., Lipton, S. A., and Sucher, N. J.: (S)NO signals: translocation, regulation, and a consensus motif. *Neuron* **18** (5): 691-6, 1997.

Standaert, D. G., Landwehrmeyer, G. B., Kerner, J. A., Penney, J. B., Jr., and Young, A. B.: Expression of NMDAR2D glutamate receptor subunit mRNA in neurochemically identified interneurons in the rat neostriatum, neocortex and hippocampus. *Brain Res Mol Brain Res* **42** (1): 89-102, 1996.

Standley, S., Roche, K. W., McCallum, J., Sans, N., and Wenthold, R. J.: PDZ domain suppression of an ER retention signal in NMDA receptor NR1 splice variants. *Neuron* **28** (3): 887-98, 2000.

Stout, C. E., Costantin, J. L., Naus, C. C., and Charles, A. C.: Intercellular calcium signaling in astrocytes via ATP release through connexin hemichannels. *J Biol Chem* **277** (12): 10482-8, 2002.

Straub, S. V., Bonev, A. D., Wilkerson, M. K., and Nelson, M. T.: Dynamic inositol trisphosphate-mediated calcium signals within astrocytic endfeet underlie vasodilation of cerebral arterioles. *J Gen Physiol* **128** (6): 659-69, 2006.

Surks, H. K.: cGMP-dependent protein kinase I and smooth muscle relaxation: a tale of two isoforms. *Circ Res* **101** (11): 1078-80, 2007.

Suzuki, N., and Hardebo, J. E.: The cerebrovascular parasympathetic innervation. *Cerebrovasc Brain Metab Rev* **5** (1): 33-46, 1993.

Takano, T., Tian, G. F., Peng, W., Lou, N., Libionka, W., Han, X., and Nedergaard, M.: Astrocyte-mediated control of cerebral blood flow. *Nat Neurosci* **9** (2): 260-7, 2006.

Tingley, W. G., Roche, K. W., Thompson, A. K., and Huganir, R. L.: Regulation of NMDA receptor phosphorylation by alternative splicing of the C-terminal domain. *Nature* **364** (6432): 70-3, 1993.

Toda, N., Uchiyama, M., and Okamura, T.: Prejunctional modulation of nitroxidergic nerve function in canine cerebral arteries. *Brain Res* **700** (1-2): 213-8, 1995.

Traynelis, S. F., Burgess, M. F., Zheng, F., Lyuboslavsky, P., and Powers, J. L.: Control of voltage-independent zinc inhibition of NMDA receptors by the NR1 subunit. *J Neurosci* **18** (16): 6163-75, 1998.

Traynelis, S. F., Hartley, M., and Heinemann, S. F.: Control of proton sensitivity of the NMDA receptor by RNA splicing and polyamines. *Science* **268** (5212): 873-6, 1995.

Triguero, D., Buciak, J., and Pardridge, W. M.: Capillary depletion method for quantification of blood-brain barrier transport of circulating peptides and plasma proteins. *J Neurochem* **54** (6): 1882-8, 1990.

Tsai, L. H., Lee, Y. J., and Wu, J. Y.: Role of N-methyl-D-aspartate receptors in gastric mucosal blood flow induced by histamine. *J Neurosci Res* **77** (5): 730-8, 2004.

Tyagi, N., Mishra, P. K., and Tyagi, S. C.: Homocysteine, hydrogen sulfide (H₂S) and NMDA-receptor in heart failure. *Indian J Biochem Biophys* **46** (6): 441-6, 2009.

Uehara, T., Nakamura, T., Yao, D., Shi, Z. Q., Gu, Z., Ma, Y., Masliah, E., Nomura, Y., and Lipton, S. A.: S-nitrosylated protein-disulphide isomerase links protein misfolding to neurodegeneration. *Nature* **441** (7092): 513-7, 2006.

Van Calker, D., Muller, M., and Hamprecht, B.: Adrenergic alpha- and beta-receptors expressed by the same cell type in primary culture of perinatal mouse brain. *J Neurochem* **30** (4): 713-8, 1978.

Vanhoutte, P. M., and Mombouli, J. V.: Vascular endothelium: vasoactive mediators. *Prog Cardiovasc Dis* **39** (3): 229-38, 1996.

Vicini, S., Wang, J. F., Li, J. H., Zhu, W. J., Wang, Y. H., Luo, J. H., Wolfe, B. B., and Grayson, D. R.: Functional and pharmacological differences between recombinant N-methyl-D-aspartate receptors. *J Neurophysiol* **79** (2): 555-66, 1998.

Viner, R. I., Williams, T. D., and Schoneich, C.: Peroxynitrite modification of protein thiols: oxidation, nitrosylation, and S-glutathiolation of functionally important cysteine residue(s) in the sarcoplasmic reticulum Ca-ATPase. *Biochemistry* **38** (38): 12408-15, 1999.

Warkentin, S., and Passant, U.: Functional imaging of the frontal lobes in organic dementia. Regional cerebral blood flow findings in normals, in patients with frontotemporal dementia and in patients with Alzheimer's disease, performing a word fluency test. *Dement Geriatr Cogn Disord* **8** (2): 105-9, 1997.

Watanabe, M., Mishina, M., and Inoue, Y.: Distinct spatiotemporal expressions of five NMDA receptor channel subunit mRNAs in the cerebellum. *J Comp Neurol* **343** (4): 513-9, 1994.

Wiencken, A. E., and Casagrande, V. A.: The distribution of NADPH diaphorase and nitric oxide synthetase (NOS) in relation to the functional compartments of areas V1 and V2 of primate visual cortex. *Cereb Cortex* **10** (5): 499-511, 2000.

Williams, K.: Ifenprodil discriminates subtypes of the N-methyl-D-aspartate receptor: selectivity and mechanisms at recombinant heteromeric receptors. *Mol Pharmacol* **44** (4): 851-9, 1993.

Wink, D. A., Kasprzak, K. S., Maragos, C. M., Elespuru, R. K., Misra, M., Dunams, T. M., Cebula, T. A., Koch, W. H., Andrews, A. W., Allen, J. S., and et al.: DNA deaminating ability and genotoxicity of nitric oxide and its progenitors. *Science* **254** (5034): 1001-3, 1991.

Wo, Z. G., and Oswald, R. E.: Unraveling the modular design of glutamate-gated ion channels. *Trends Neurosci* **18** (4): 161-8, 1995.

Wood, M. W., VanDongen, H. M., and VanDongen, A. M.: Structural conservation of ion conduction pathways in K channels and glutamate receptors. *Proc Natl Acad Sci U S A* **92** (11): 4882-6, 1995.

Wyllie, D. J., Behe, P., and Colquhoun, D.: Single-channel activations and concentration jumps: comparison of recombinant NR1a/NR2A and NR1a/NR2D NMDA receptors. *J Physiol* **510 (Pt 1)**: 1-18, 1998.

Yamakura, T., and Shimoji, K.: Subunit- and site-specific pharmacology of the NMDA receptor channel. *Prog Neurobiol* **59** (3): 279-98, 1999.

Yang, Y., Ge, W., Chen, Y., Zhang, Z., Shen, W., Wu, C., Poo, M., and Duan, S.: Contribution of astrocytes to hippocampal long-term potentiation through release of D-serine. *Proc Natl Acad Sci U S A* **100** (25): 15194-9, 2003.

Yao, Y., and Mayer, M. L.: Characterization of a soluble ligand binding domain of the NMDA receptor regulatory subunit NR3A. *J Neurosci* **26** (17): 4559-66, 2006.

Yoon, H. J., Cho, S. W., Ahn, B. W., and Yang, S. Y.: Alterations in the activity and expression of endothelial NO synthase in aged human endothelial cells. *Mech Ageing Dev* **131** (2): 119-23, 2010.

Zonta, M., Angulo, M. C., Gobbo, S., Rosengarten, B., Hossmann, K. A., Pozzan, T., and Carmignoto, G.: Neuron-to-astrocyte signaling is central to the dynamic control of brain microcirculation. *Nat Neurosci* **6** (1): 43-50, 2003.

Zukin, R. S., and Bennett, M. V.: Alternatively spliced isoforms of the NMDAR1 receptor subunit. *Trends Neurosci* **18** (7): 306-13, 1995.